Four-fold Differential Measurement of the Drell-Yan Cross Section

PhD Defence

Craig Wells
Freiburg, 16.05.2025

Underlying Physics

The Standard Model of Particle Physics

The Standard Model describes three (of four) fundamental forces: strong force, weak force and electromagnetism.

Quarks

Carry colour and (fractional) electric charge.

Cannot be observed as isolated particles.

Combine to form nuclei of atoms.

Leptons

Carry electric charge.

Can exist as free particles.

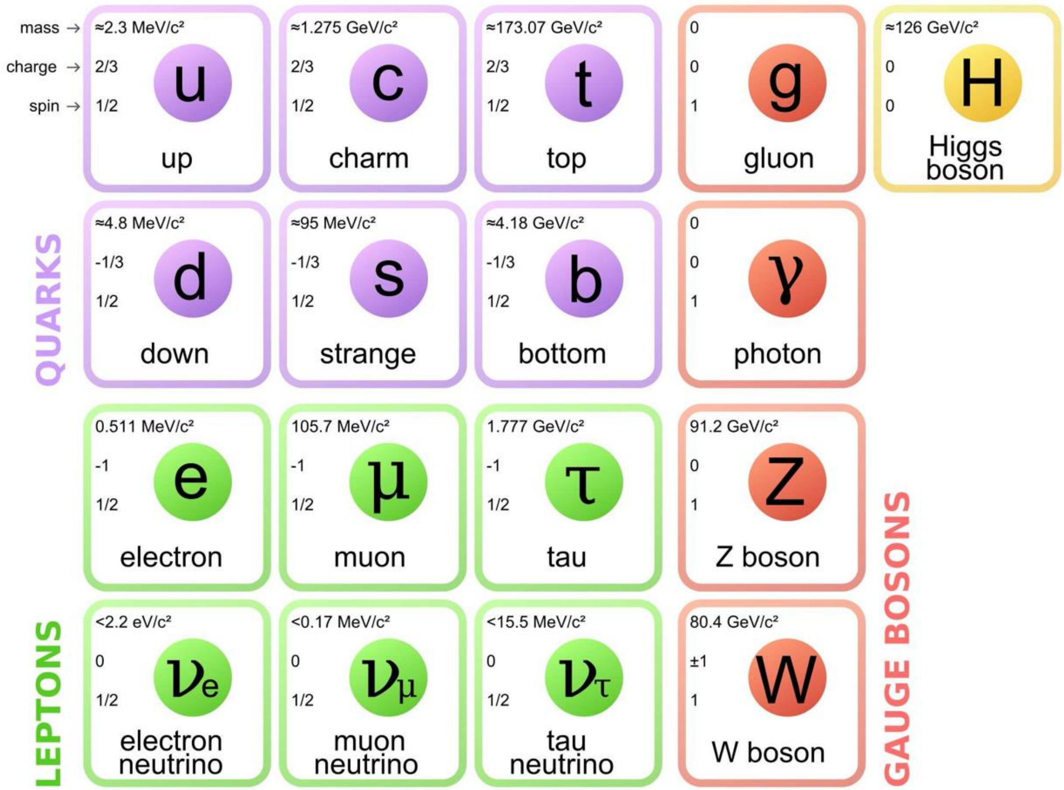

Higgs boson

Provides mass to elementary particles through electroweak spontaneous symmetry breaking.

Gauge bosons

Mediate interactions between different particle types.

Also **antimatter**: quantum charge conjugated versions of each particle. Very rarely observed naturally in nature.

The Standard Model of Particle Physics

Unanswered Questions

- In 2012, the Higgs boson was discovered and the Standard Model was complete.
- Many open questions are still unanswered:
  - How does gravity function at a quantum level?
  - Why is there an observed imbalance between matter and antimatter?
  - What is the source of dark matter and dark energy?
  - What is the origin of the neutrino mass?
  - Many others!
- Two possible ways to answer these questions:
  - Look directly for new physics beyond the Standard Model (BSM).
  - Measure the parameters and processes of the Standard Model at extremely high levels of experimental precision and compare to the theoretical values.

The Drell-Yan Process

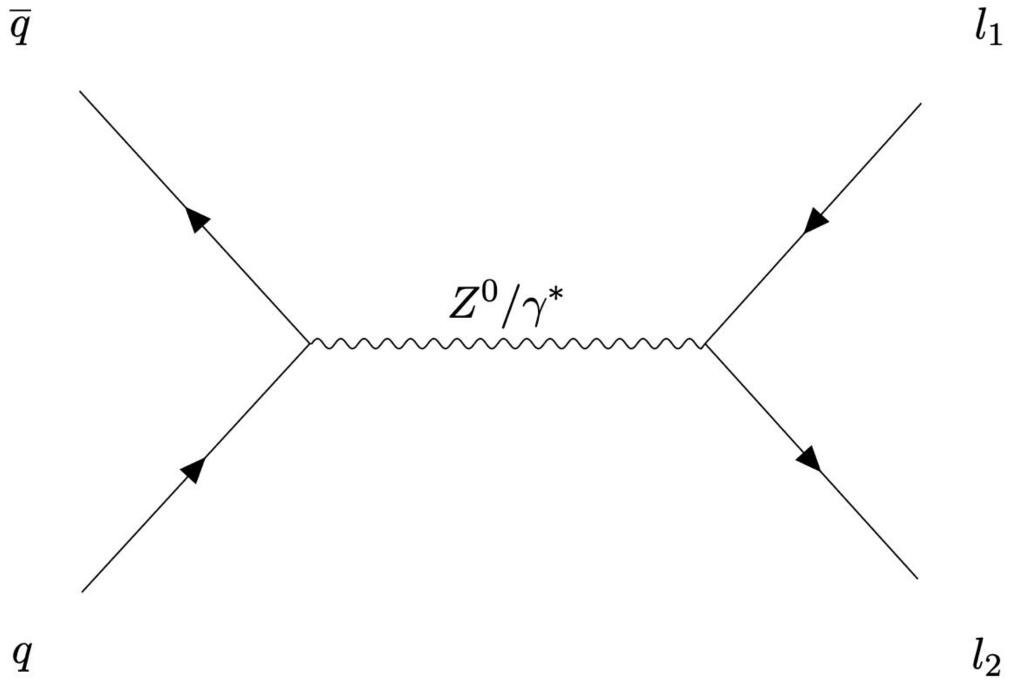

- The process of producing a lepton pair from a quark/antiquark pair was first theorised by Sidney Drell and Tung Mow Yan in 1970.
- In the Standard Model, this process can be mediated by the W or Z bosons or an off-shell photon.
  - Consider only the Z/γ^* mediated process for this analysis.
- This process can be used to study many different aspects of particle physics (electroweak, QCD, PDFs, new physics etc).

The Drell-Yan Process

$$\frac{d\sigma}{dp_T^Z\, dy^Z\, dm^Z\, d\cos\theta\, d\phi} = \frac{3}{16\pi}\frac{d\sigma^{U+L}}{dp_T^Z\, dy^Z\, dm^Z}$$
$$\left\{\boxed{(1+\cos^2\theta)} + \boxed{\frac{1}{2}A_0(1-3\cos^2\theta) + A_1\ \sin 2\theta\ \cos\phi}\right.$$
$$\boxed{+\frac{1}{2}A_2\ \sin^2\theta\ \cos 2\phi + A_3\ \sin\theta\ \cos\phi} + \boxed{A_4\ \cos\theta}$$
$$\left.\boxed{+A_5\ \sin^2\theta\ \sin 2\phi + A_6\ \sin 2\theta\ \sin\phi + A_7\ \sin\theta\ \sin\phi}\right\}.$$

LO

NLO

NNLO

- The full five-fold differential cross section can be decomposed into a set of 8 angular coefficients, 9 harmonic polynomials and an unpolarised cross section.
  - Decomposition holds in the rest frame of the mediating boson. Choose the Collins-Soper frame for convenience.
- The angular coefficients are unitless ratios of helicity cross sections i.e how much each spin state contributes to the overall cross section.
- Allows for the separation of the boson kinematics (angular coefficients) and the angular dependence of the decay products (harmonic polynomials).

Goal 1: Measure these angular coeffcients for the Z boson double differentially in the full lepton phase space.

The Weak Mixing Angle

- The SU(2) x U(1) symmetry of the electroweak theory predicts the existence of four distinct bosons:
  - B_μ from U(1)
  - W_μ^a (a = 1,2,3) from SU(2)

- To recover the physically observed $W^\pm$, Z and γ bosons:

$$W^\pm = \frac{1}{\sqrt{2}}\left(W_\mu^1 \mp i\, W_\mu^2\right)$$

$$\begin{pmatrix} Z \\ \gamma \end{pmatrix} = \begin{pmatrix} \cos\theta_W & -\sin\theta_W \\ \sin\theta_W & \cos\theta_W \end{pmatrix} \begin{pmatrix} W_\mu^3 \\ B_\mu \end{pmatrix}$$

- θ_W: Weak mixing angle, one of the fundamental parameters of the Standard Model!
- To incorporate higher perturbative orders into the weak mixing angle, define the effective leptonic weak mixing angle:

$$\sin^2\theta_{eff}^l = \kappa_l \sin^2\theta_W$$

From the Drell-Yan process to the Weak Mixing Angle

Forwards-Backwards Asymmetry

$$\frac{d\sigma}{dp_T^Z\, dy^Z\, dm^Z\, d\cos\theta\, d\phi} = \frac{3}{16\pi} \frac{d\sigma^{U+L}}{dp_T^Z\, dy^Z\, dm^Z}$$

$$\left\{ \boxed{(1+\cos^2\theta)} + \boxed{\frac{1}{2} A_0 (1 - 3\cos^2\theta) + A_1 \sin 2\theta \cos\phi} \right.$$

$$+ \boxed{\frac{1}{2} A_2 \sin^2\theta \cos 2\phi + A_3 \sin\theta \cos\phi} + \boxed{A_4 \cos\theta}$$

$$\left. + \boxed{A_5 \sin^2\theta \sin 2\phi + A_6 \sin 2\theta \sin\phi + A_7 \sin\theta \sin\phi} \right\}.$$

LO

NLO

NNLO

- The Z boson is an electroweak boson ⇒ conservation of parity must be violated!
- Parity violation is encoded in the A_3, A_4, and A_7 coefficients.
  - Theory predictions show that the effects of A_3 and A_7 are very small.

- Parity violation manifests as more Z events produced forwards ($\cos\theta_{CS} > 0$) than backwards ($\cos\theta_{CS} < 0$)
  - Forwards-backwards asymmetry (A_{FB})
  - $\boxed{A_{FB} = \frac{3}{8} A_4}$

From the Drell-Yan process to the Weak Mixing Angle

Linking A_{FB} to $sin^2\theta_W$

Forwards-Backwards Asymmetry

$$A_{FB} = \frac{3}{8} A_4$$

$$A_{FB} = A_{FB}(v_l, a_l)$$

(Effective) Weak Mixing Angle

$$\sin^2\theta^l_{eff} = \kappa_l \sin^2\theta_W$$

$$\sin^2\theta^l_{eff} = \frac{1}{4}(1 - \frac{v_l}{a_l})$$

- A_{FB} and $\sin^2\theta^l_{eff}$ are both related through the vector and axial couplings.
- Measuring A_4 also allows for the weak mixing angle to be measured!

Goal 2: Estimate the potential sensitivity to the weak mixing angle through a measurement of A_4.

Choice of Decay Channels

- Four channels where the angular coefficients can be measured:
  - $Z \rightarrow e^+e^-$ ($|Y_Z| < 2.4$), ee_{CC}
  - $Z \rightarrow \mu^+\mu^-$ ($|Y_Z| < 2.4$), $\mu\mu_{CC}$
  - $Z \rightarrow e^+e^-$ ($1.2 < |Y_Z| < 3.6$), ee_{CF}
  - $Z \rightarrow \tau^+\tau^-$
- Disregard the τ channel entirely.
  - Hadronic resolution worse than electromagnetic resolution.
  - Resolution on missing energy is even worse.
  - Not suitable for a precison analysis!
- Forward electrons require further calibration efforts before they can be used for data analysis.
  - Use them only for estimating the sensitivity to the weak mixing angle.

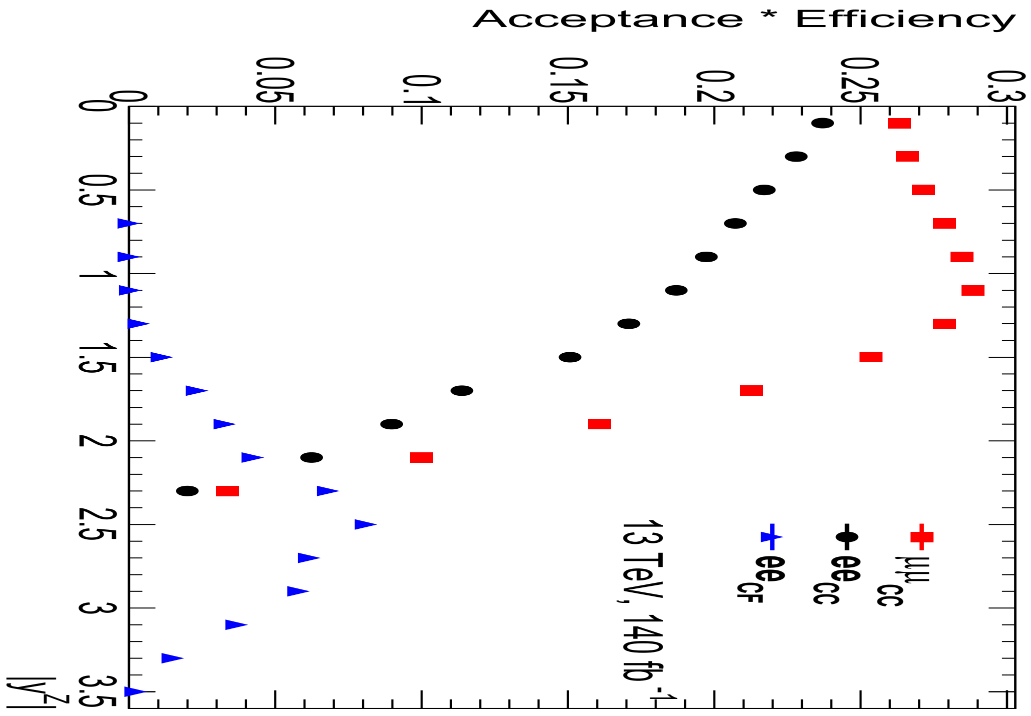

Experimental Setup

The Large Hadron Collider (LHC)

- The LHC is a 27km long proton-proton particle collider, operated by CERN in Switzerland.

- Its second data taking campaign (Run 2) from 2015 – 2018 saw protons colliding at a centre of mass energy of 13 TeV.

- The resultant collisions are detected at four points corresponding to four particle detectors:
  - ALICE
  - LHCb
  - CMS
  - ATLAS

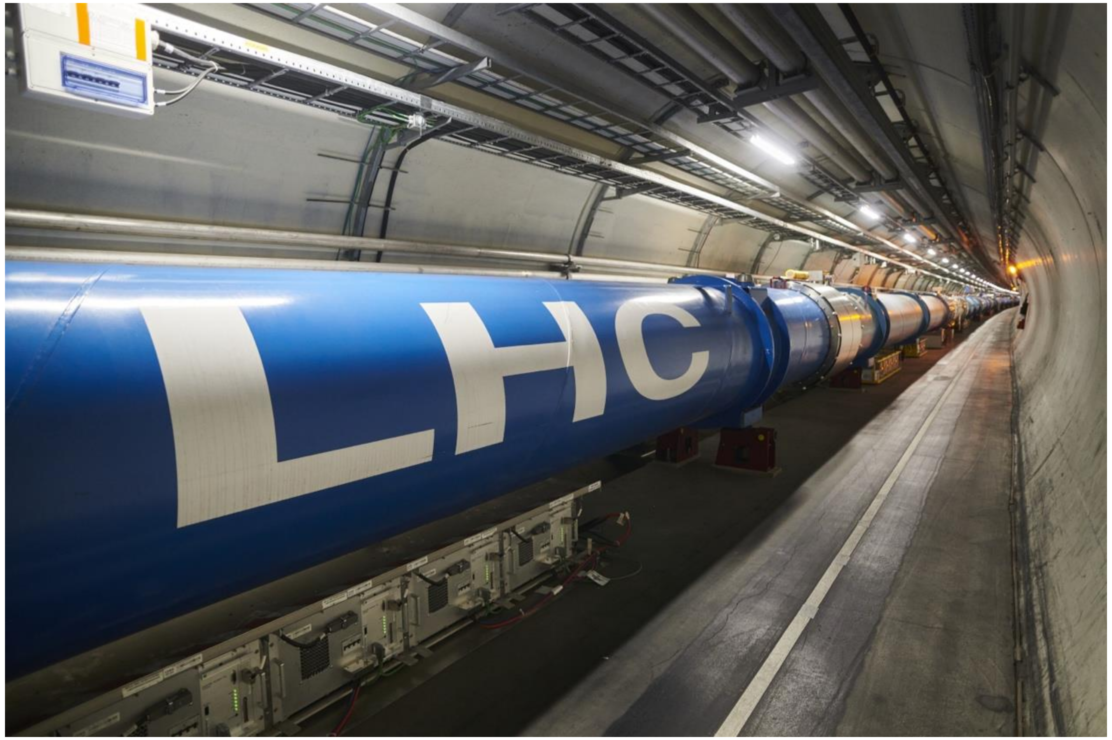

The ATLAS Experiment

Central Region - $|\eta| < 2.5$

- ATLAS is a general purpose particle detector at the LHC.
- Layered structure providing almost 4π solid angle coverage
  - Silicon tracker measuring position and momentum of charged particles.
  - Liquid argon calorimeters to measure particle energies.
  - Dedicated muon tracking system to improve particle identification.
- Trigger system to select the most interesting events.
  - LHC collides protons at 40 MHz.
  - ATLAS records approximately 1 kHz.

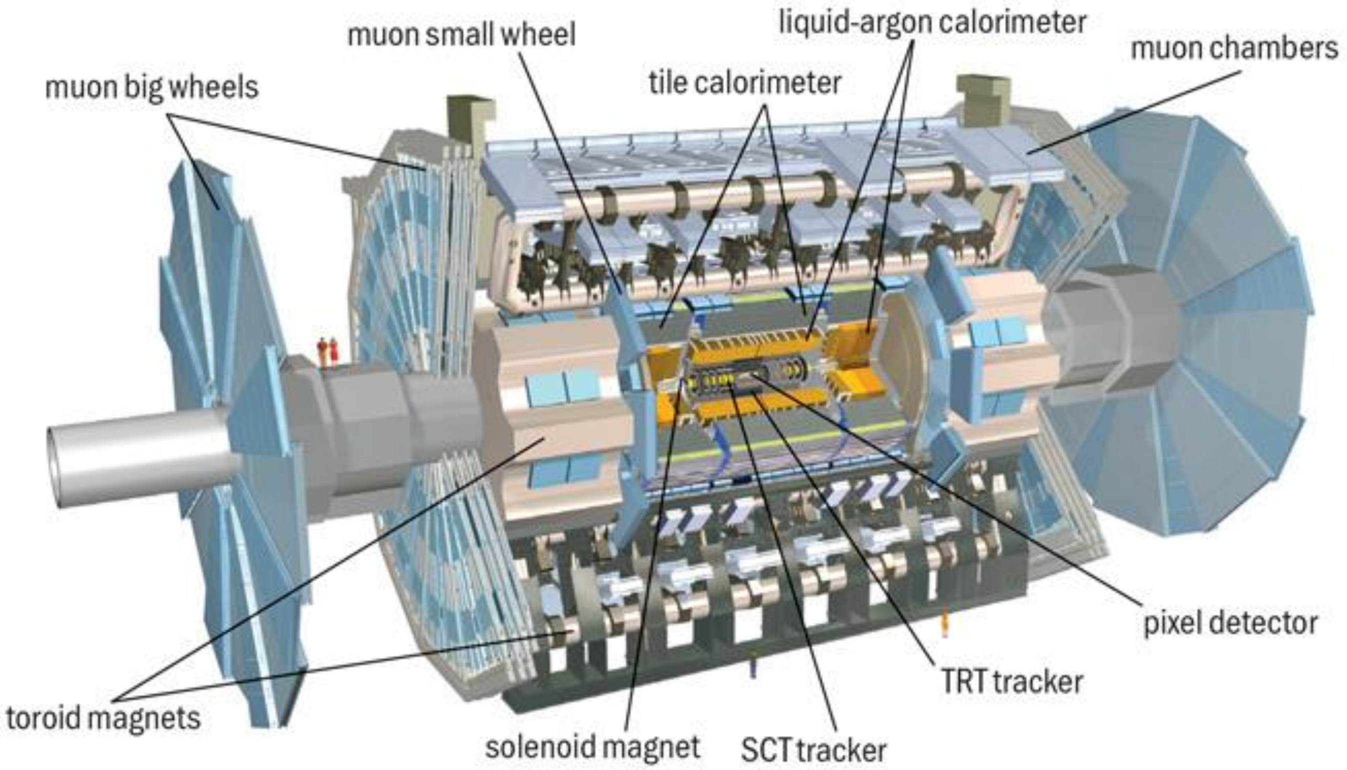

The ATLAS Experiment

Forward Region - 2.5 < |η| < 4.9

- Two electromagnetic calorimeters cover the region 2.5 < |η| < 4.9 :
  - Electromagnetic Endcap Inner Wheel (EMEC)
  - Forward Calorimeter (FCal)

- Many challenges to working in the forward region!
  - Larger calorimeter cell sizes
  - No tracking coverage.
  - Much higher amount of passive material.

- Forward electrons are not officially calibrated by ATLAS.
  - Develop our own calibration chain!

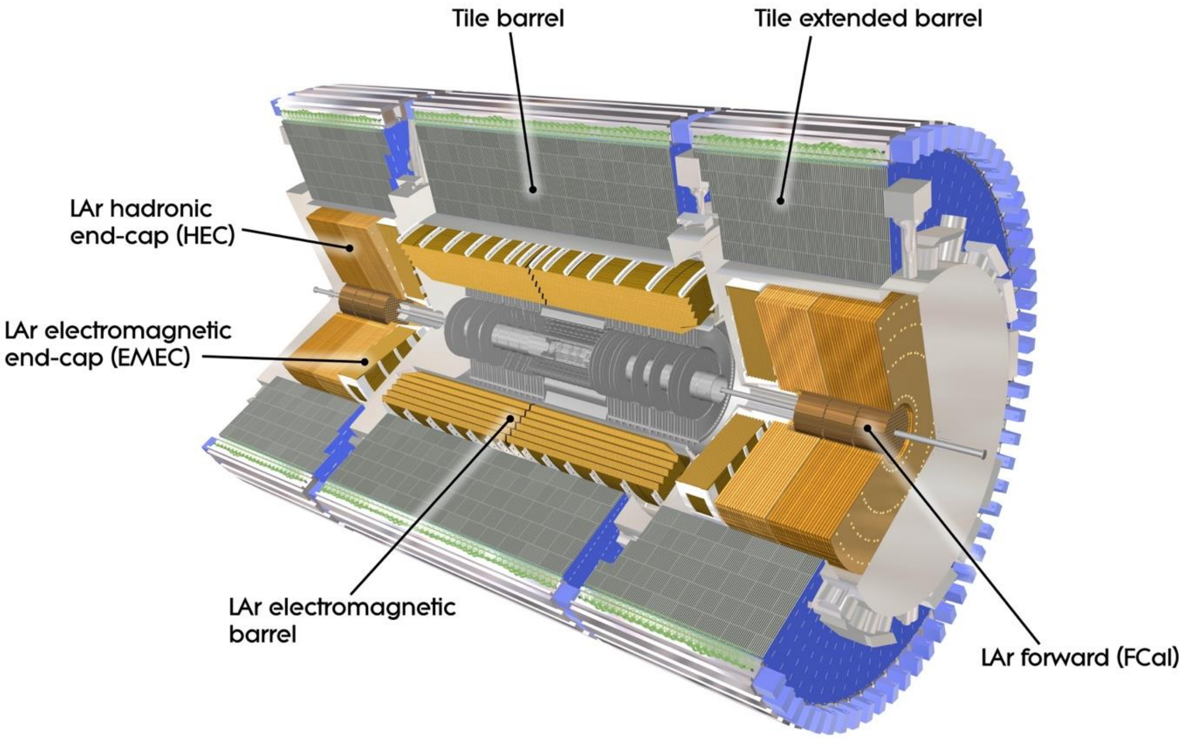

Forward Electron Calibration

Forward Electron Calibration

Calibration Chain

Harmonising the response of the calorimeter cells.

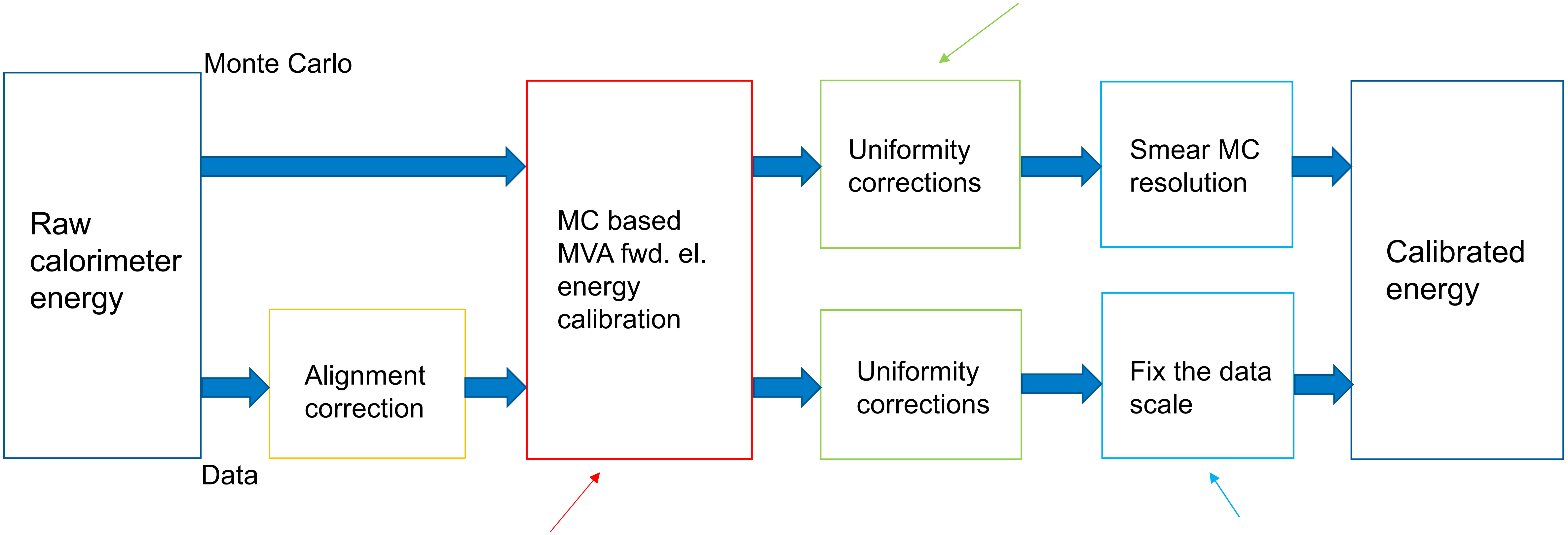

Moving the reconstructed energy to the true energy.

Matching the Z mass spectra in data and simulation.

The calibration chain was completely redeveloped for $\sqrt{s}$ = 13 TeV to maximise the sensitivity to the weak mixing angle!

Forward Electron Calibration

MVA Calibration - Introduction

- Use a multivariate analysis (MVA) to predict the ratio of E_{true}/E_{reco} and use this as a correction to the reconstructed energy i.e:

$$E_{Calibrated} = \frac{E_{true}}{E_{reco}} \times E_{reco}$$

- For the MVA, use an ensemble of boosted decision trees that follow the detector geometry:
  - EMEC, Transtion Region and FCal

- Use training variables that cover the following points:
  - How energetic was the electron?
  - What is the position of the electron in the detector?
  - What were the pileup conditions when the electron was detected?
  - How did the electromagnetic shower develop in the calorimeter?

Forward Electron Calibration

MVA Calibration - Results

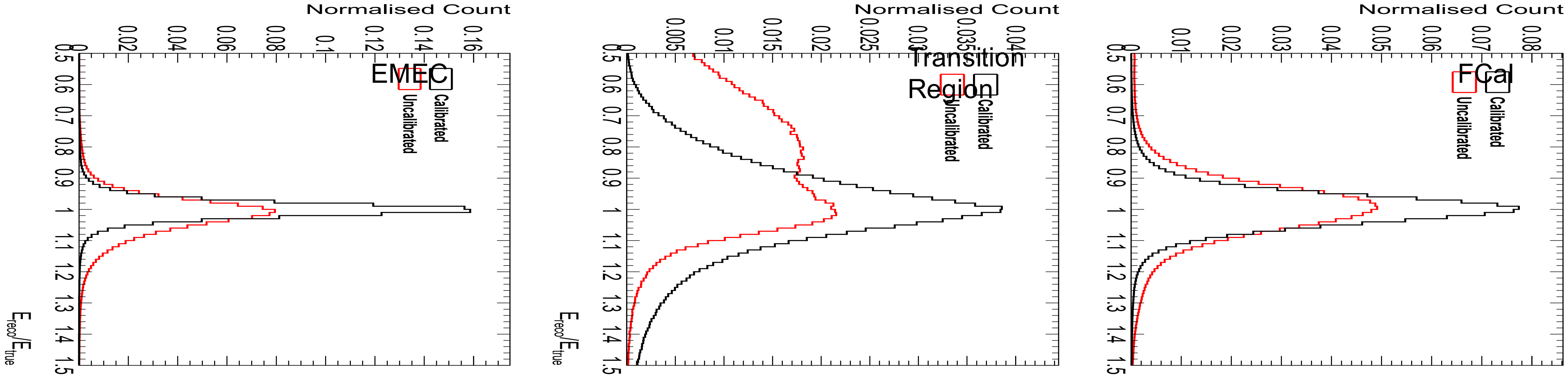

- The MVA calibration is highly successful with big improvements in the E_{reco}/E_{true} distribution:
  - Scale (position of the peak)
  - Resolution (spread of the distribution)

- Improvements are not only inclusive but also across phase space!
  - Approximate 40% improvement in the forward electron resolution.
  - Translates to a 20% (10%) improvement in the Z resolution in CF events in Monte Carlo (data).

Forward Electron Calibration

MVA Calibration - Results

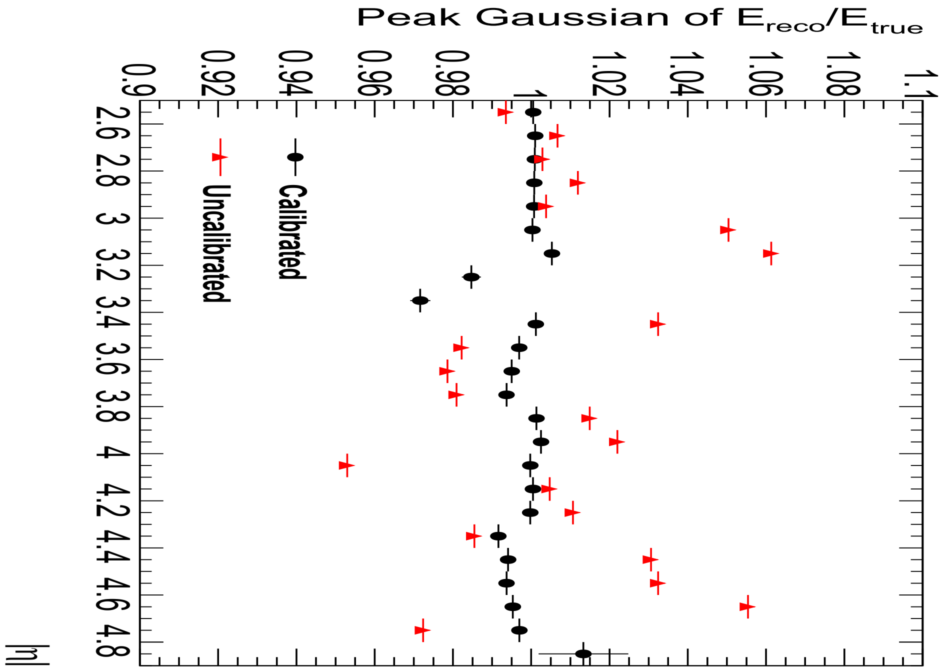

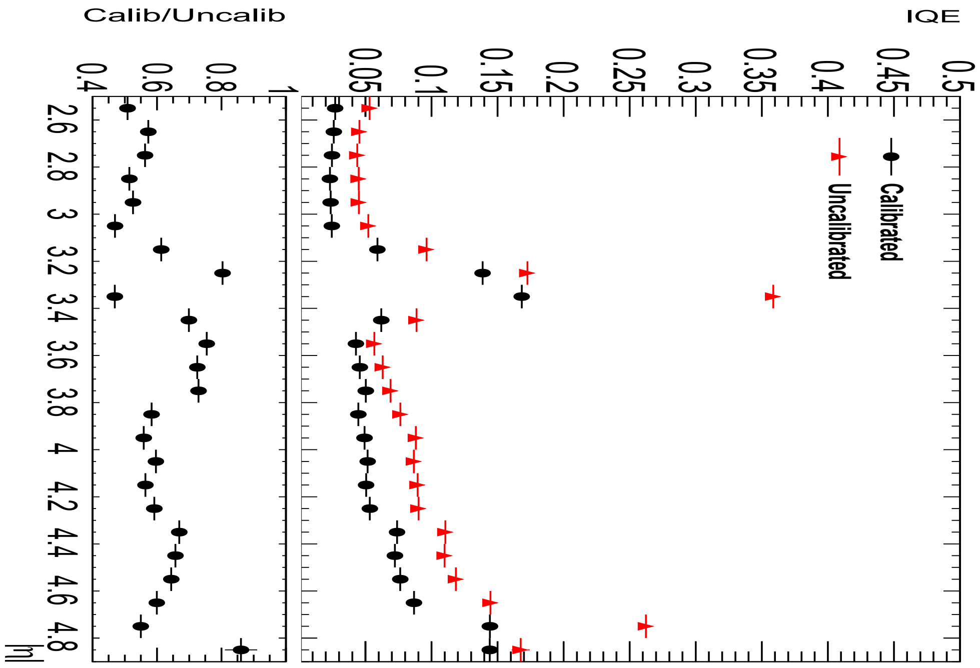

- The MVA calibration is highly successful with big improvements in the E_{reco}/E_{true} distribution:
  - Scale (position of the peak)
  - Resolution (spread of the distribution)

- Improvements are not only inclusive but also across phase space!
  - Approximate 40% improvement in the forward electron resolution.
  - Translates to a 20% (10%) improvement in the Z resolution in CF events in Monte Carlo (data).

Forward Electron Calibration

In Situ Calibration - Introduction

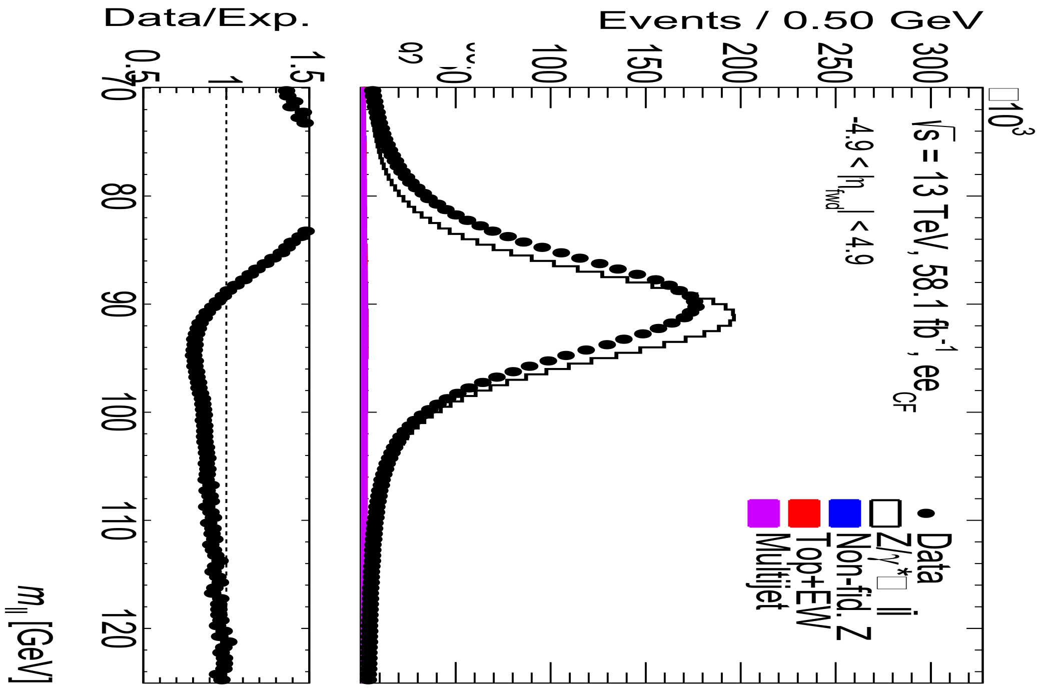

- Post-MVA and uniformity corrections show clear differences between the data and Monte Carlo distributions.
- Align the data and Monte Carlo mass spectra by:
  - Smearing the Monte Carlo to match the resolution in data
  - Shifting the data distribution to match the peak in Monte Carlo

Forward Electron Calibration

In Situ Calibration – Fit Process

- In order to derive the corrections, use a double sided crystal ball (DSCB) function with parameters that model the data.
  - Gaussian core with two power-law tails.
- Convolve the DSCB with the signal Monte Carlo (T_S) and add in background processes (T_B) to form a template.

$$Template = \ DSCB \ \otimes T_S + T_B$$

- Fit the template to the data i.e optimise the parameters of the DSCB.
- Smear the Monte Carlo → Generate random (x,y) points on the post-fit DSCB and multiply the electron energy by the x value.

$$E_{Smeared} = E_{Monte\ Carlo} \ \times \ (1 + x)$$

- Shift the data → Use the mean (μ) of the post-fit DSCB as a uniform shift to the electron energy.

$$E_{Shifted} = E_{Data} \ \times \ \frac{1}{1 + \mu}$$

Forward Electron Calibration

In Situ Calibration - Results

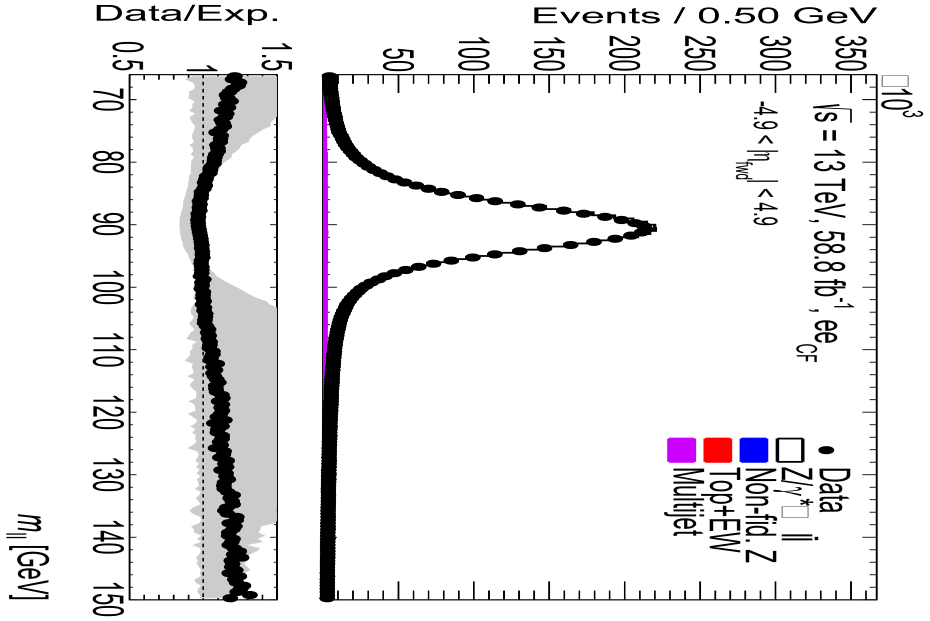

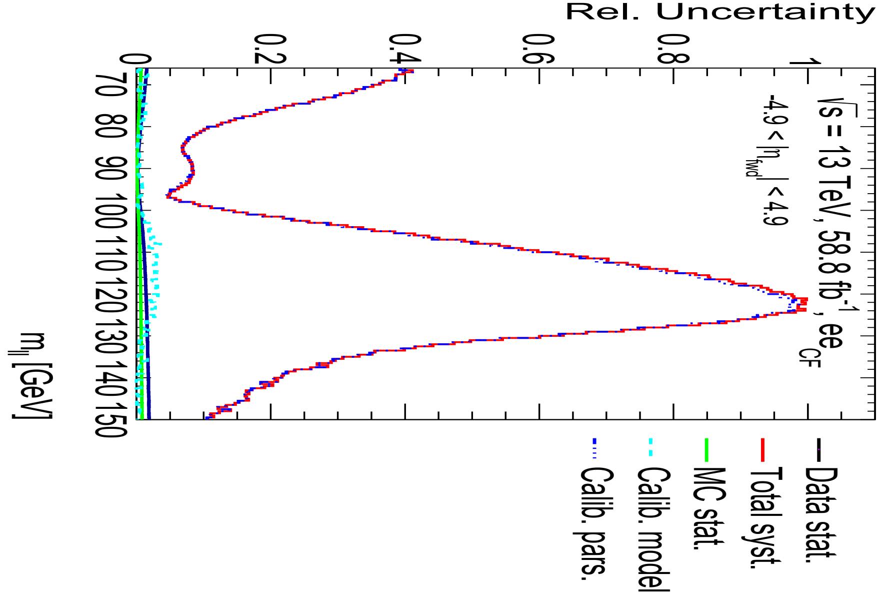

- Post-calibration, the nominal agreement of the data and Monte Carlo is very good!
  - On pole, agreement is almost perfect.
  - Lower and upper tails very sensitive to small changes → agreement worsens.

- Lower and upper tails also display very high levels of uncertainty due to large errors in the calibration parameters.
  - The calibration is therefore a significant systematic uncertainty when using forward electrons for physics analysis.

Angular Coeffcient Results

Signal Region Definition

Analysis Cuts and Binning

- A precision measurement requires a signal region that is extremely pure in signal → apply cuts to the lepton parameters to minimise the number of background events!

ee_{CC} Channel

- Two electrons with $|\eta| < 2.4$
  - Exclude $1.37 < |\eta| < 1.52$
- $p_T > 22$ GeV
- $80 < m_{ee} < 102$ GeV
- $|z_0| < 0.5$ mm
- Significance $(|z_0|) < 5$
- Pass medium identification

$\mu\mu_{CC}$ Channel

- Two muons with $|\eta| < 2.4$
- $p_T > 20$ GeV
- $80 < m_{\mu\mu} < 102$ GeV
- $|z_0| < 0.5$ mm
- Significance $(z_0) < 3$

For both channels, use a high granularity analysis binning that spans the ranges:

- $|Y_Z|$: 0 – 2.4 (6 uniform bins)
- $p_{T,Z}$: 0 – 6500 GeV (25 asymmetric bins)

Control Plots

Electron Channel

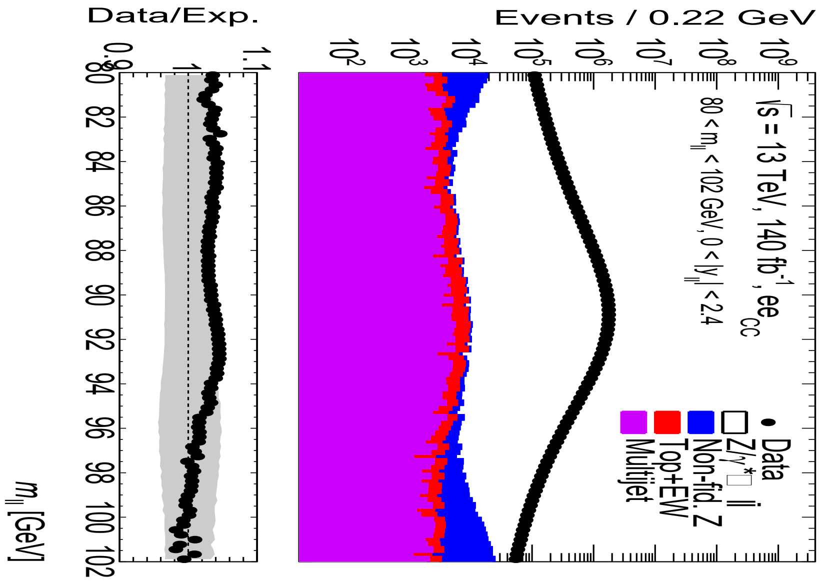

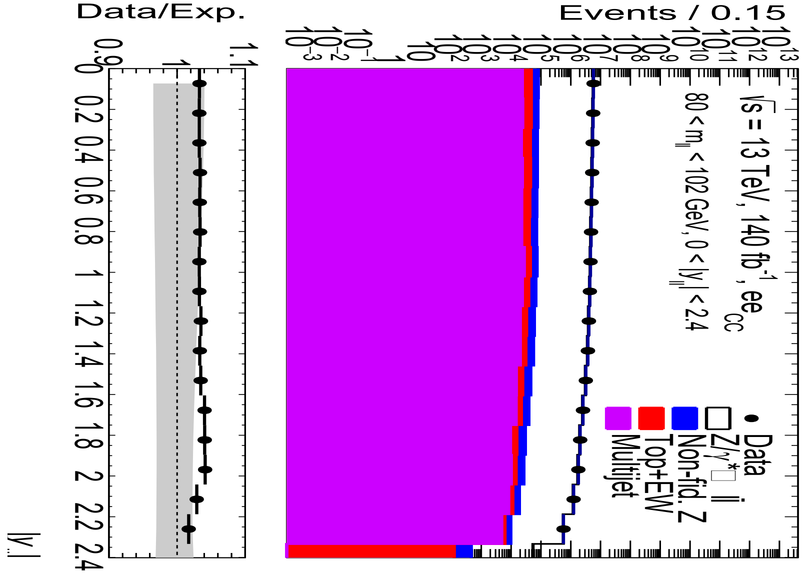

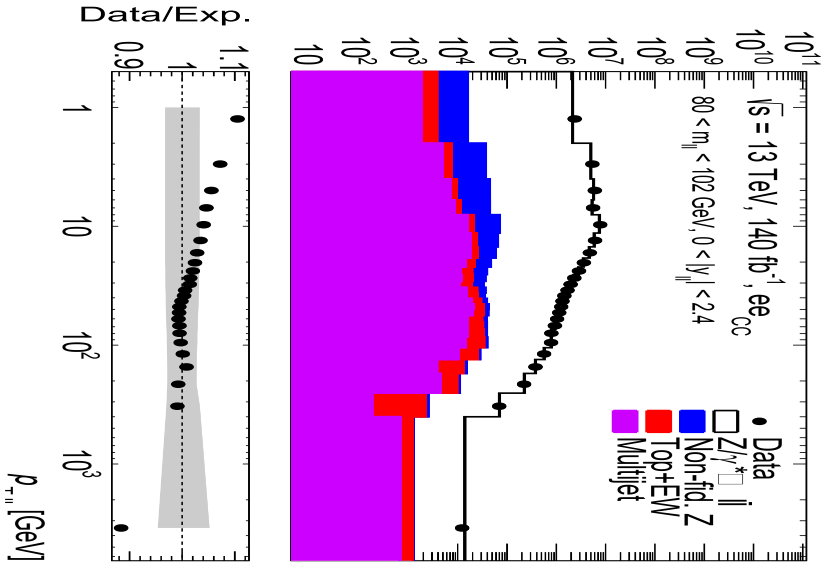

- Control plots show a very pure signal region, with low amounts of background.
  - Total background events ~1.5% of the total number of events.

- Good agreement between data and the simulation means the angular coefficients can be extracted from this region.
  - Z transverse momentum is heavily affected by higher order QCD effects not accounted for by the signal Monte Carlo which affects the agreement with the data for this variable.

- Should expect the greatest statistical sensitivity at low rapidity and low Z transverse momentum.

Individual Channels

Uncertainty Breakdowns – Unpolarised Cross Section

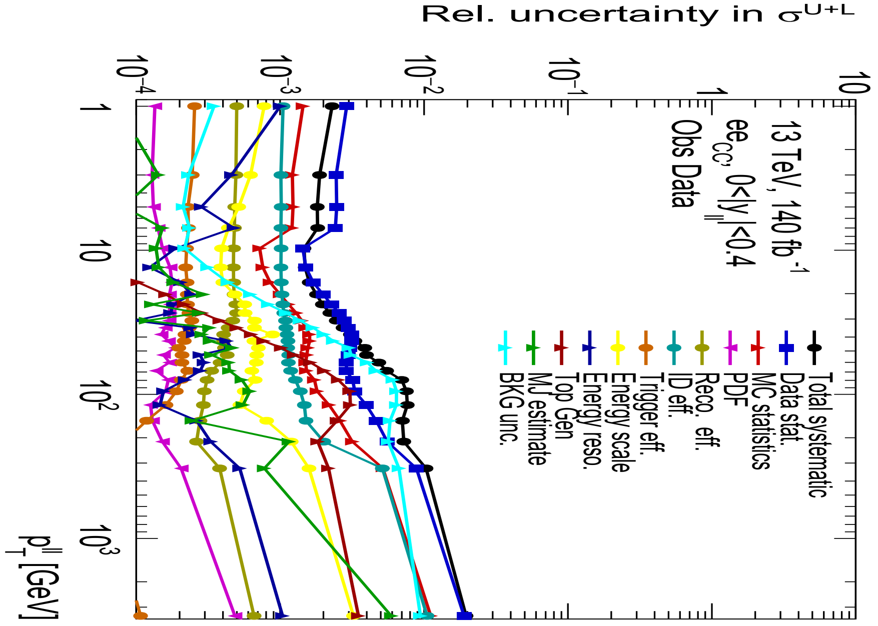

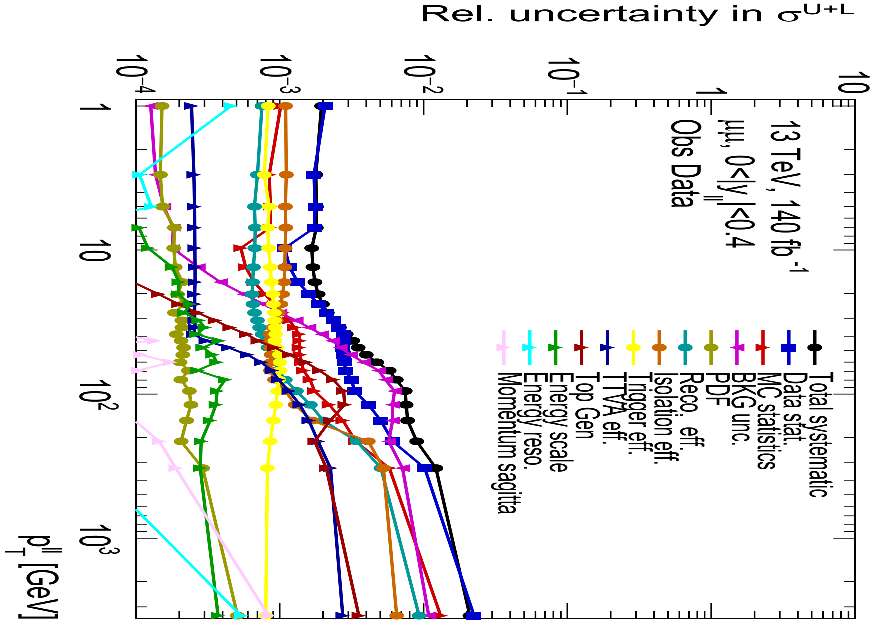

- Extremely high levels of precision reached in both the electron and muon channels!
  - Better than percent level precision across most of phase space!
  - Same level of precision in a single rapidity bin as in the entire rapidity integrated 8 TeV measurement!

- Spike in background related systematics become dominant at $p_{T,Z}$ = 100 GeV
  - BKG uncertainty: +/- 20% variation on amount of background.
  - Top Gen: Differences between Monte Carlo generators.
  - Background processes become on-shell in this region causing increase in uncertainty.

- Very high level of measurement granularity means statistical uncertainties are otherwise dominant.

Individual Channels

Uncertainty Breakdowns – Angular Coefficients

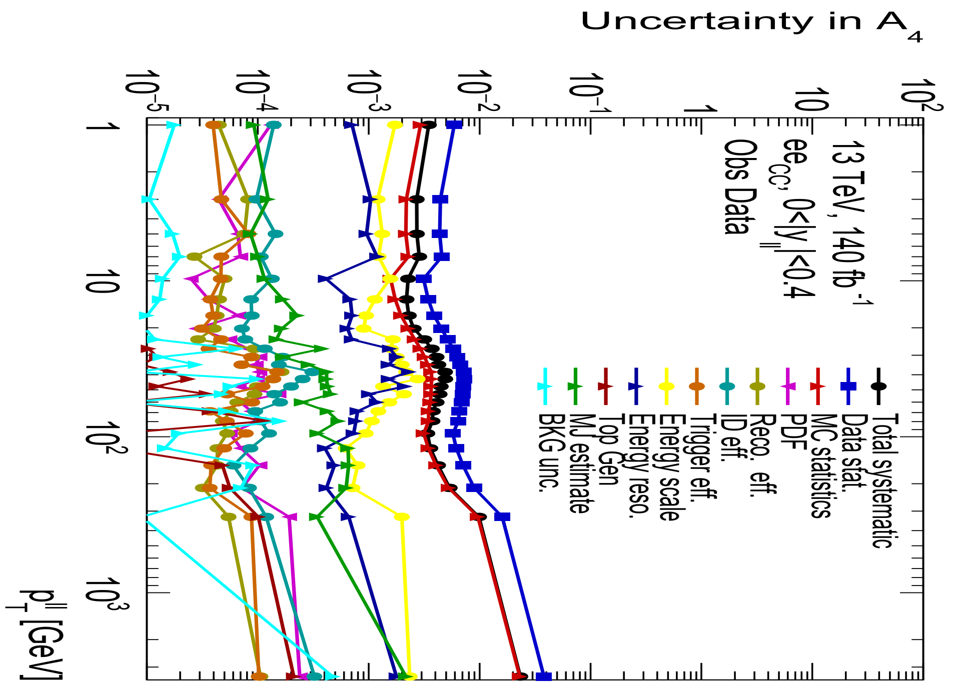

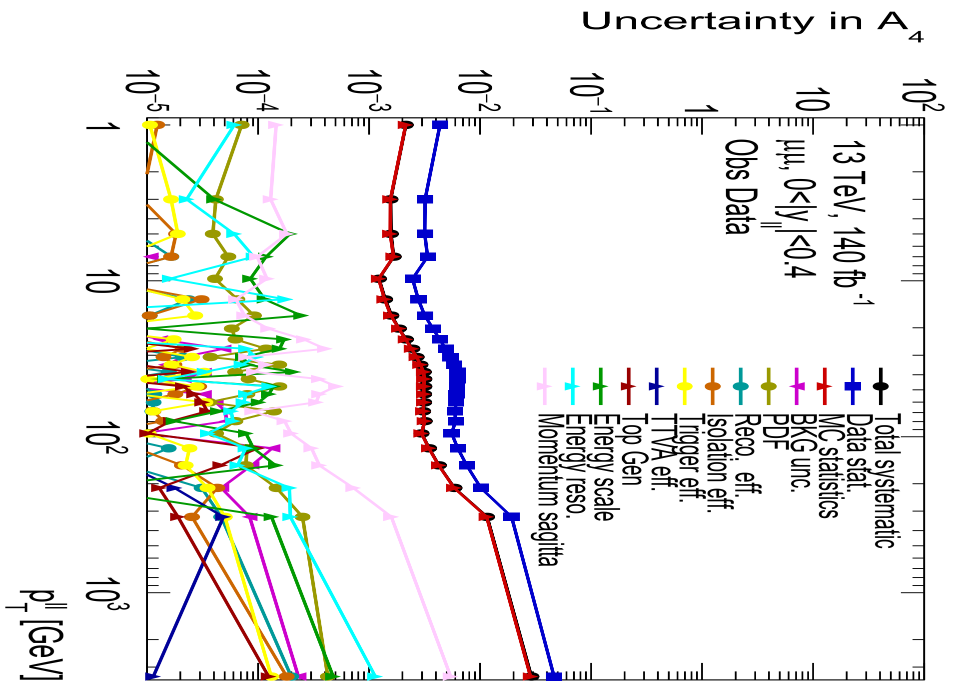

- Statistical uncertainties dominate for the angular coefficients as well.
- Calibration systematics become more important for the electron channel.
- Muon channel completely statistically dominated, all other systematic groups are of a similar magnitude.

Electron and Muon Channel Agreement

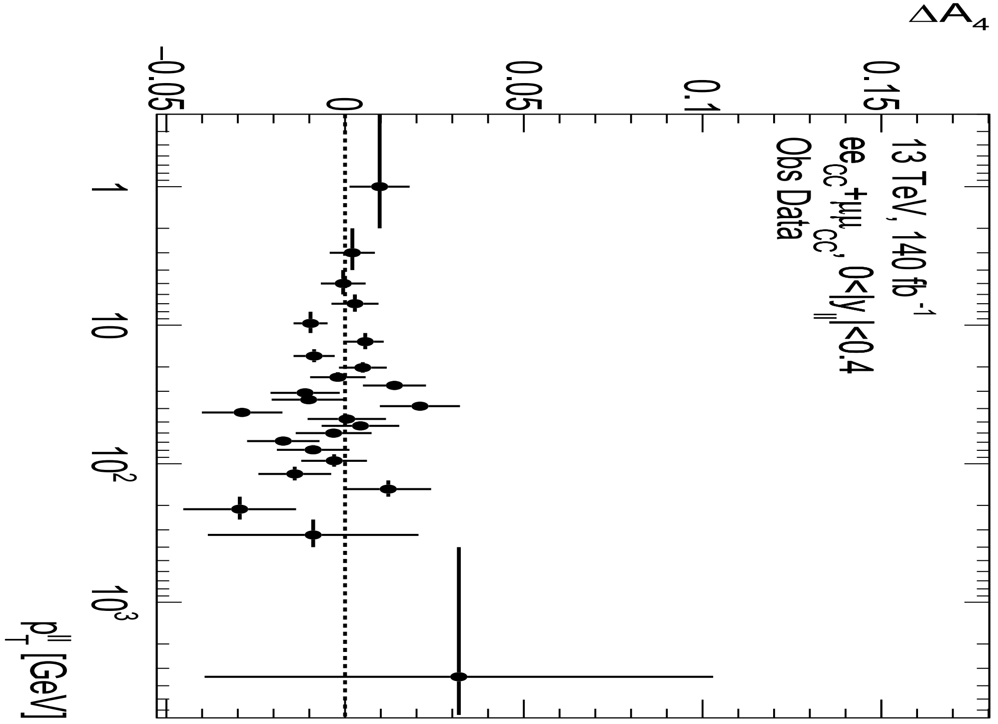

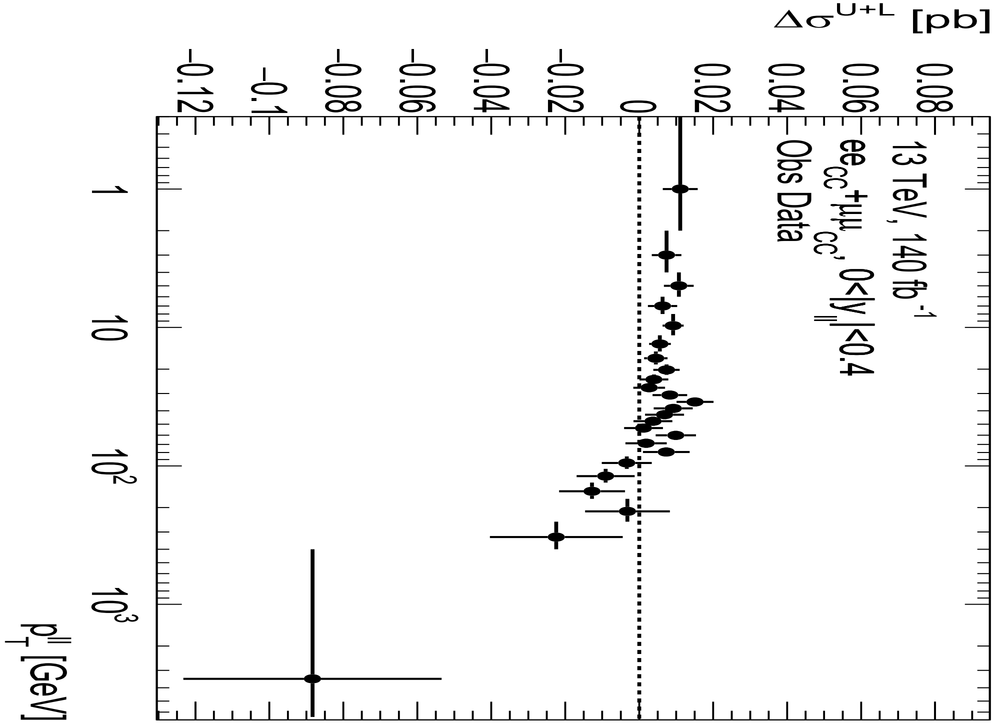

- Before combining the two channels to improve statistical sensitivity, the agreement must be checked.
  - Lepton flavour universality → Should be no difference between the electron and muon channels.

$$\Delta A_i = \frac{A_{i,ee} - A_{i,\mu\mu}}{A_{i,ee}}$$

- Angular coefficients show good agreement with zero!

- Small disagreement of ~1% at low $p_{T,Z}$ for the unpolarised cross section.
  - Most likely due to an issue with the trigger scale factor in the muon channel.

Angular Coefficients

A_0

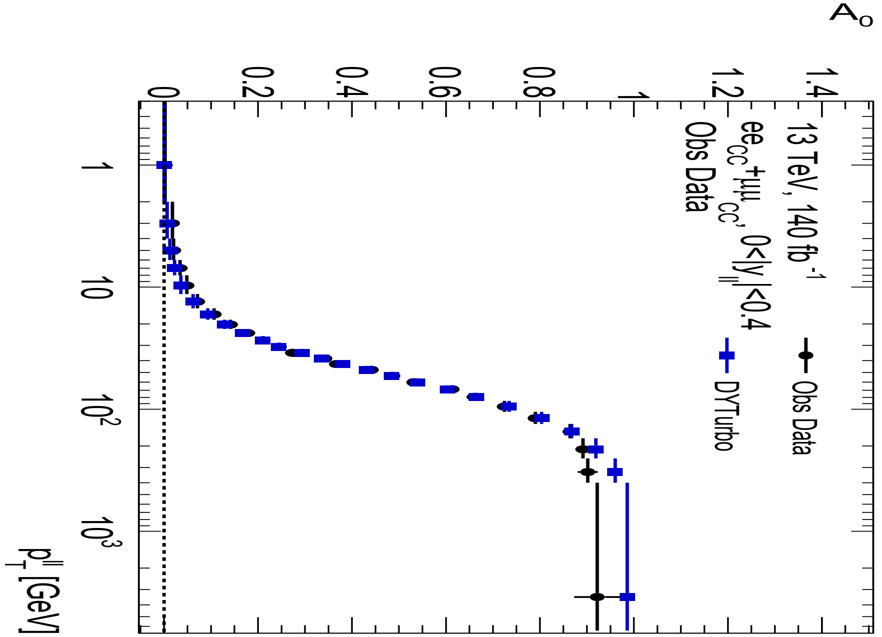

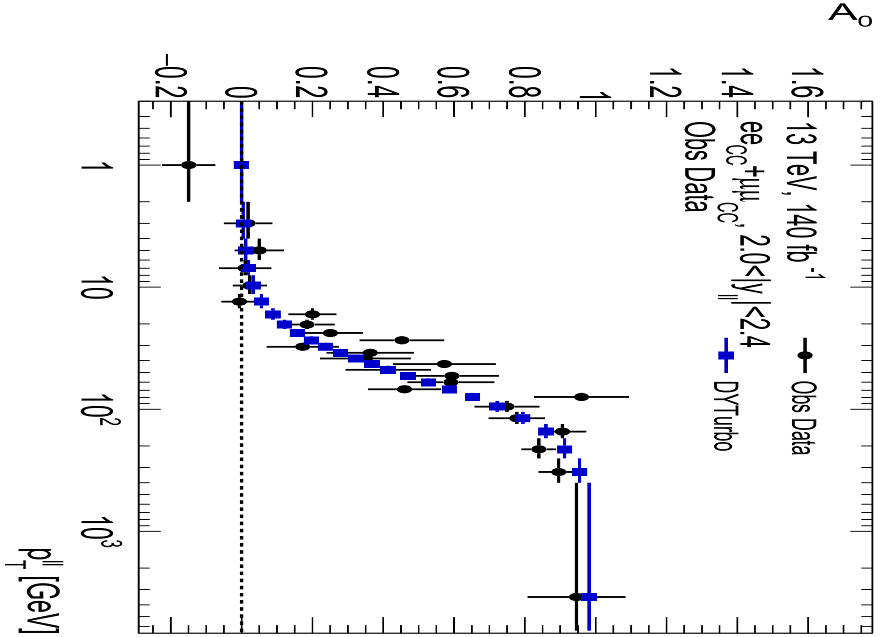

- DYTurbo: NNLO fixed order calculation of the angular coefficients.
  - Value chosen to be zero in the 0 – 2 GeV bin.

- Observed values match the prediction very closely until the high $p_{T,Z}$ region.
  - Higher perturbative orders necessary to more accurately replicate the data.

- No deviations from the Standard Model.

Angular Coefficients

A_2

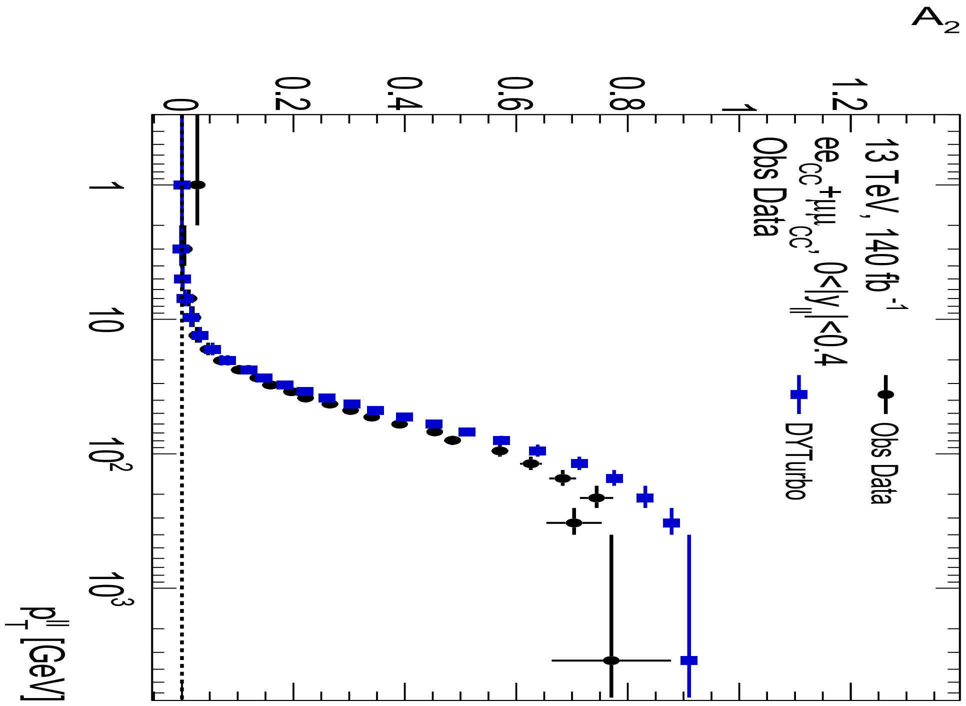

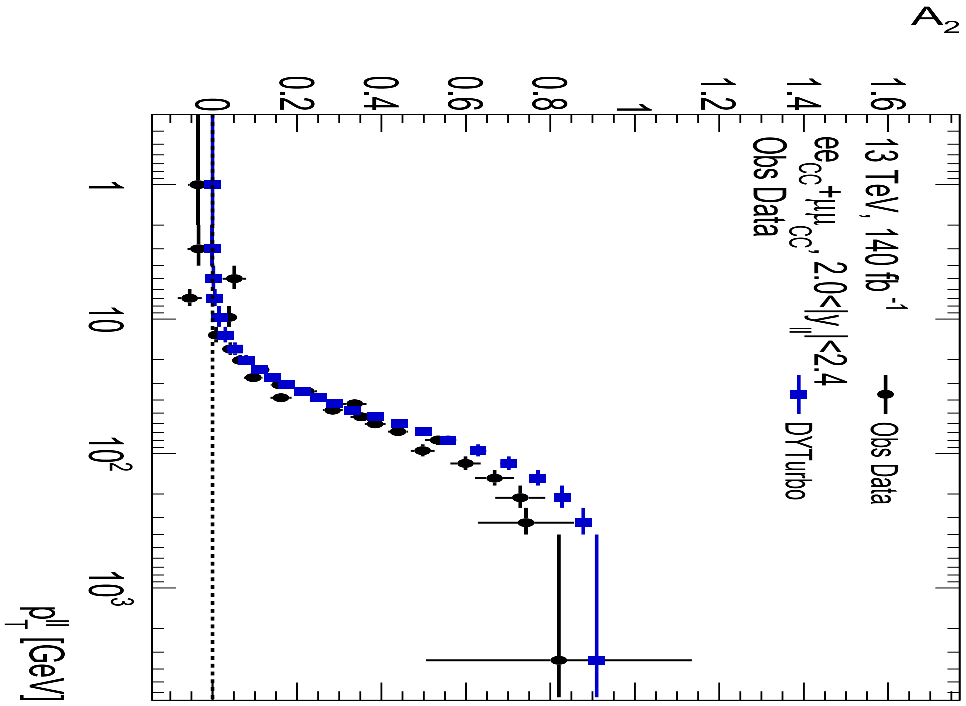

- Non-zero A_2 is observed in the first $p_{T,Z}$ bin at both low and high rapidity.
  - Expected to be approximately zero.
  - Non-zero behaviour may be due to QCD vacuum effects or transverse momentum dependent PDFs (amongst other possible mechanisms).

- Still to early to say whether this is evidence of new physics → more statistical precision necessary.

- This non-zero behaviour has also been previously by ATLAS and by LHCb.

Angular Coefficients

A_4 - Results

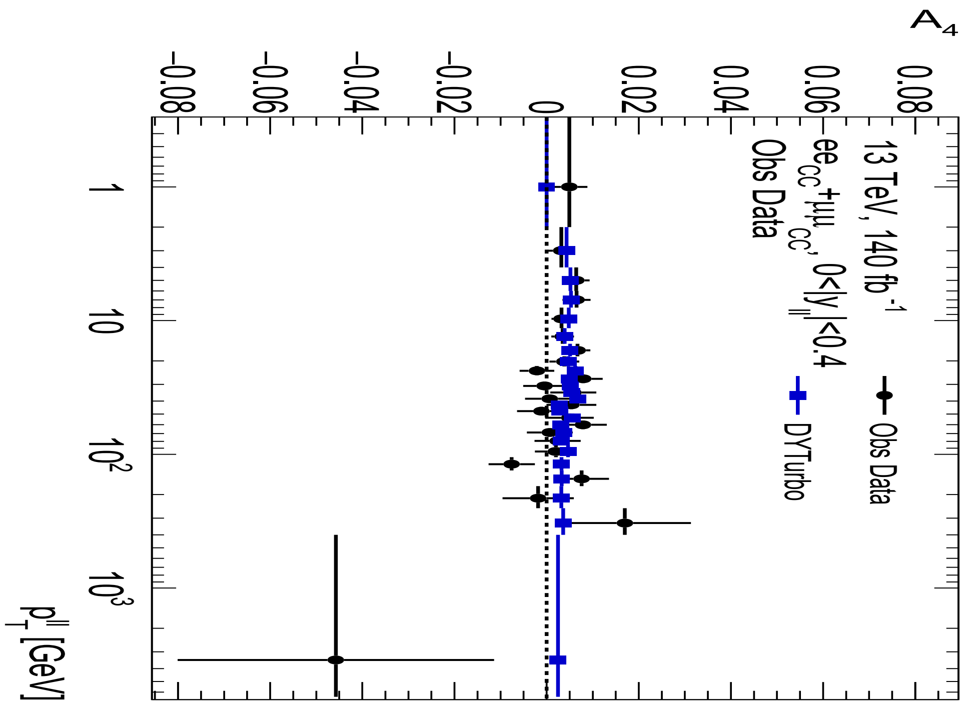

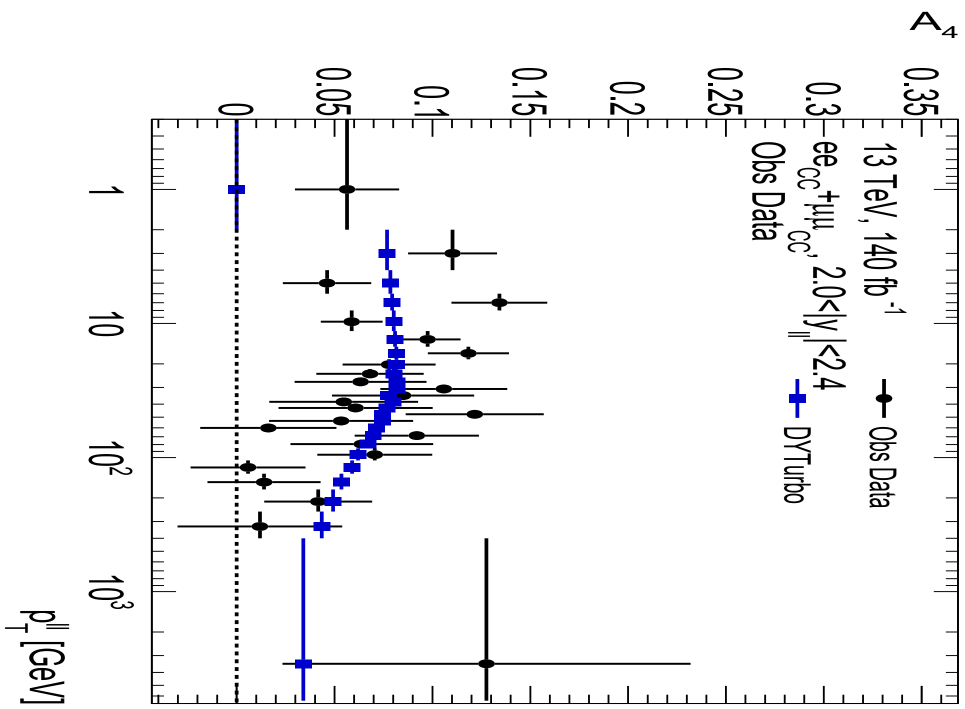

- Magnitude of A_4 is directly proportional to the boson rapidity.
  - A_4 is a proxy for the forwards-backwards asymmetry so this is expected!

- Z p_T is mainly a QCD effect → pure EW parity violation is “masked” at higher momentum values.

Angular Coefficients

Unpolarised Cross Section - Results

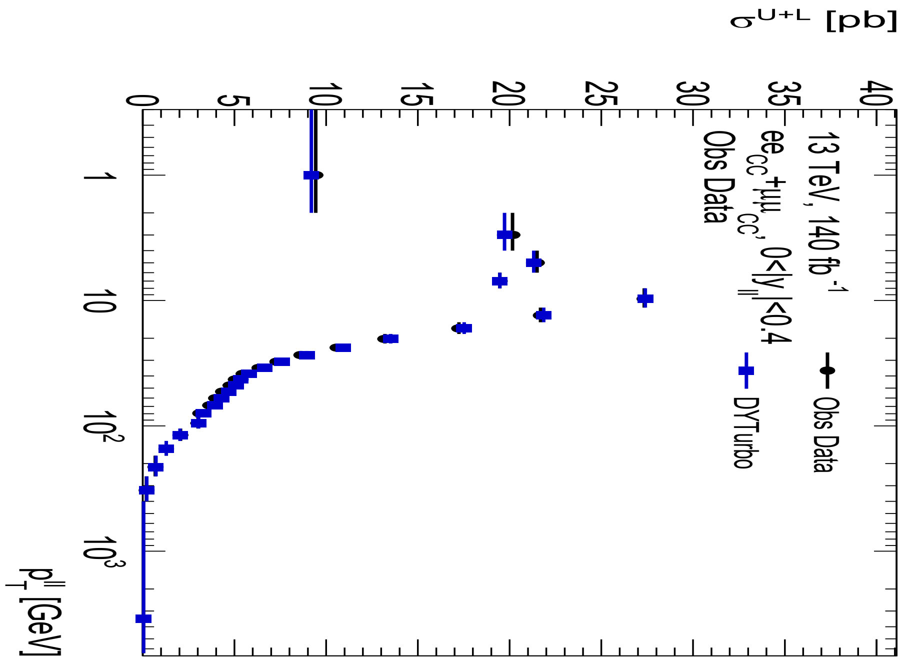

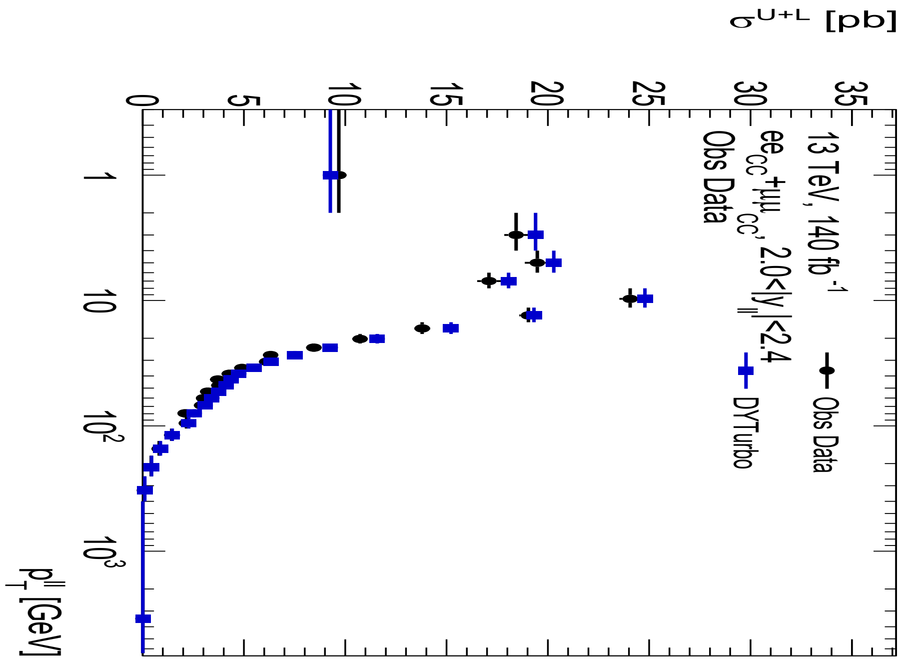

- Very good agreement with the Standard Model at low rapidity.
- Larger degree of disagreement at high rapidity likely due to missing higher order corrections in DYTurbo.
  - No evidence of new physics as the disagreement is still relatively small.

Angular Coefficients

Lam-Tung Relation

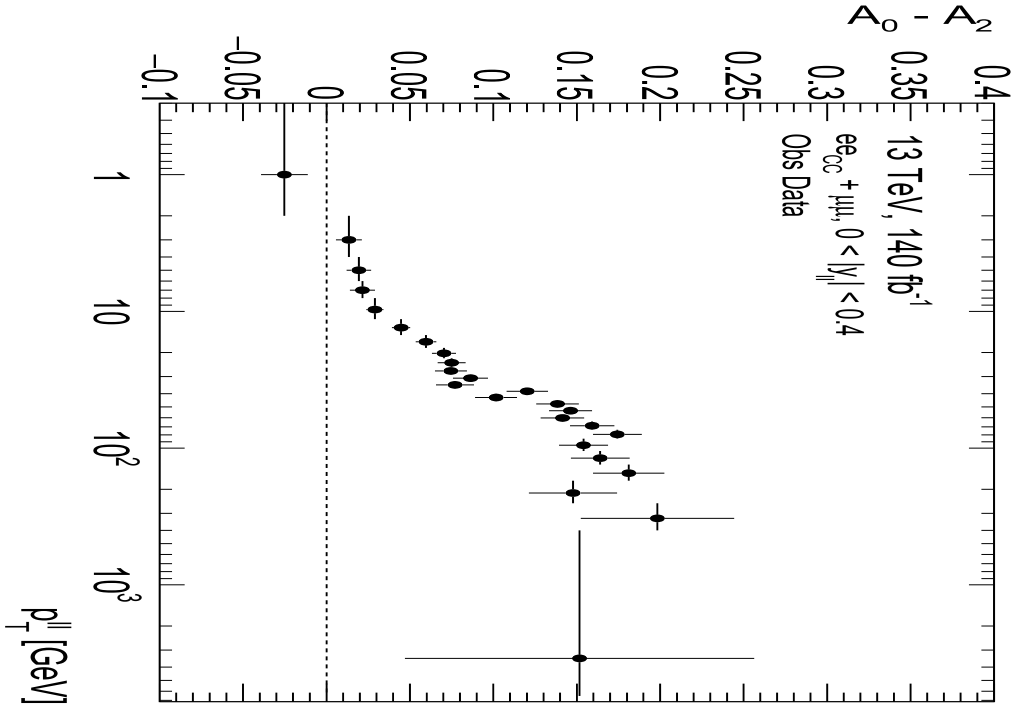

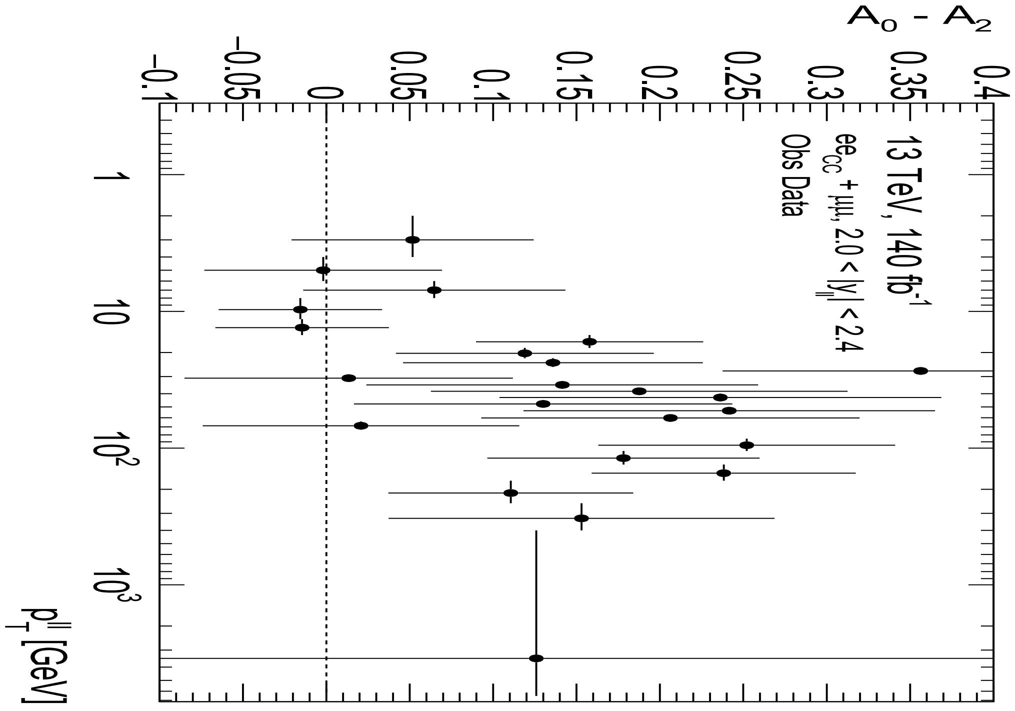

- Lam-Tung relation states that $A_0 - A_2 = 0$ at leading order:
  - Violated when QCD interactions are considered.

- Clear violation of the Lam-Tung relation is seen at lower rapidities, with decreasing statistical sensitivity as rapidity increases.

- No experimental sensitivity to the violation in the highest rapidity bin.

Sensitivity to $sin^2\theta_W$

Maximising Sensitivity to A_4

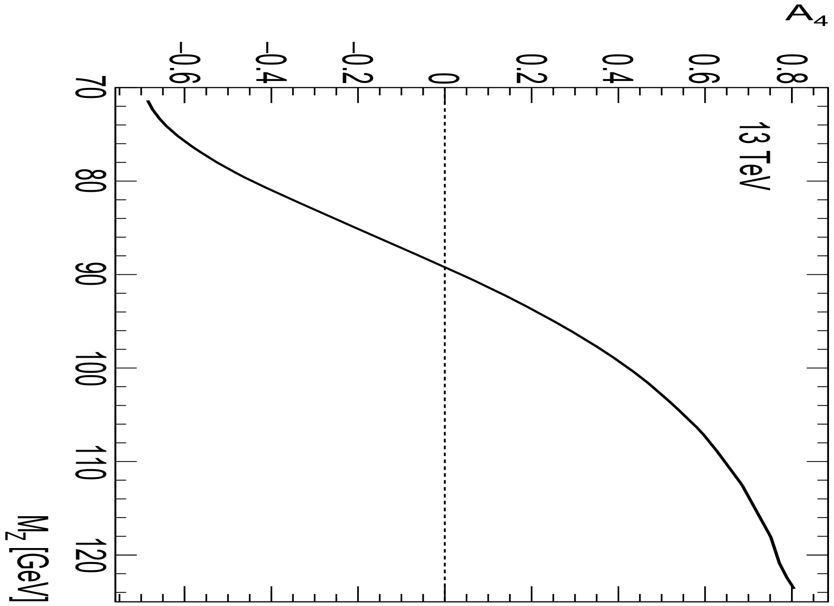

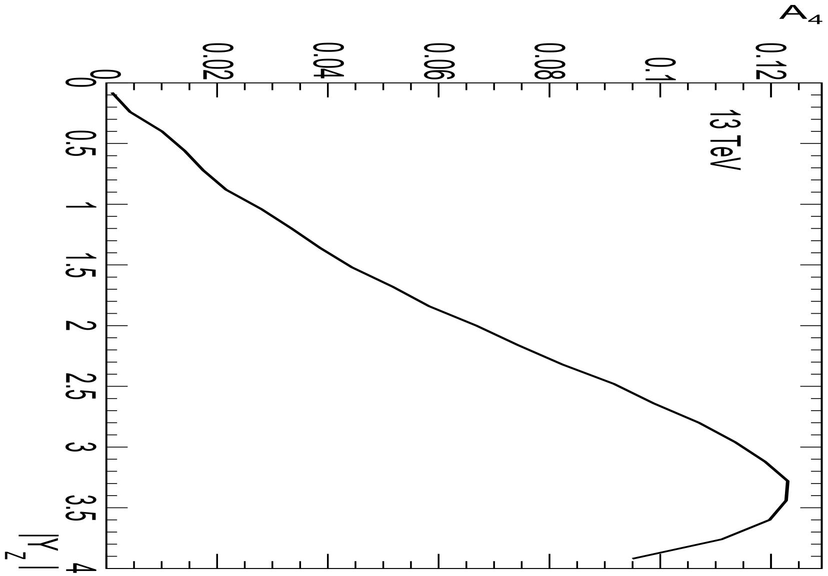

- $A_{FB} = 0$ exactly on the Z pole but becomes non-zero through interference with photon mediated interactions.

- At hadron colliders it is impossible to know the origin of the incoming quark/antiquark ⇒ assume the Z is boosted in the direction of the quark.
  - Crucial assumption for A_{FB} since this defines what “forward” and “backward” is.
  - At high rapidity values, there is less ambiguity in this definition and greater statistical sensitivity.

- Modify the analysis binning to reflect this:
  - M_{ll}: 70 – 80 – 100 – 125 GeV
  - Y_{ll}: 0 – 3.6 in 9 uniform bins.
  - $p_{T,Z}$: inclusive

A_4 Results

CF Channel

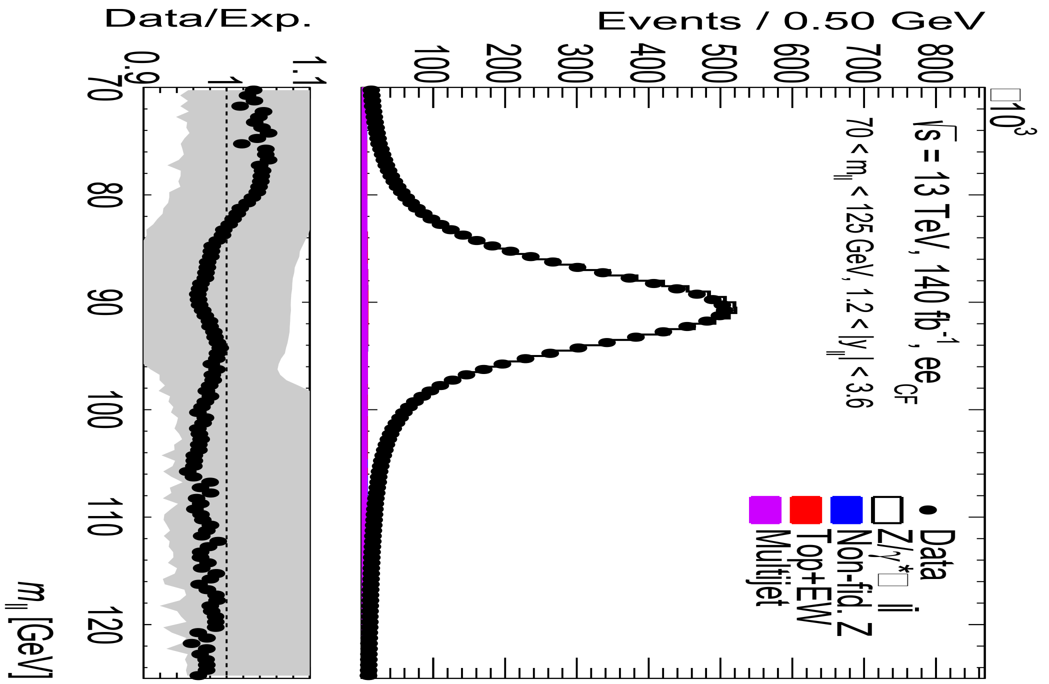

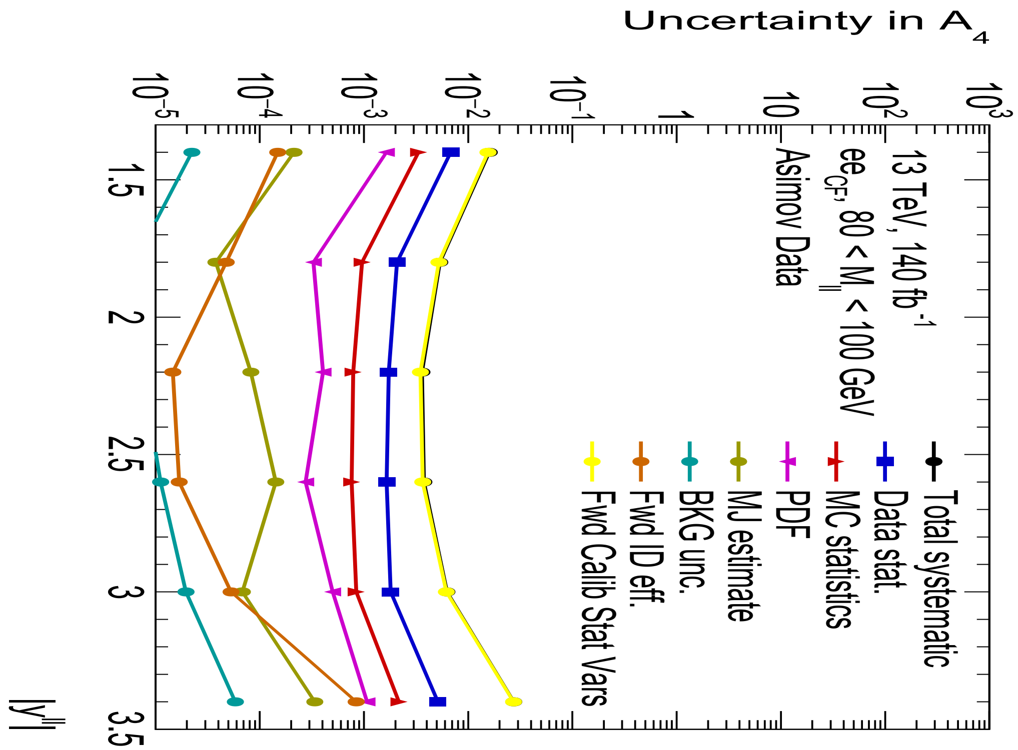

- Forward electron calibration produces an excellent agreement between the data and Monte Carlo for the nominal case!
  - Not yet finalised so the final weak mixing angle value cannot be extracted → perform an Asimov study to estimate the final uncertainty.
- In the CF channel, consider only systematic variations on the forward electron.
- As is expected the forward calibration is the largest source of uncertainty.
  - Otherwise statistically limited.

Translating to $sin^2\,\theta_{eff}^{l}$ Sensitivity

- Using the xFitter framework, the uncertainties in A_4 from the covariance matrix can be propagated to an uncertainty in the weak mixing angle.
  - The extraction is done at LO in QCD.

- Combining the three channels and using the NNPDF 4.0 PDF set, the estimated sensitivity is:

$$\sin^2\theta_{eff}^{l} = 0.23152\ \pm 0.00022\ (stat) \pm 0.00010\ (systematic) \pm 0.00014\ (theory)$$

$$\sin^2\theta_{eff}^{l} = 0.23152\ \pm 0.00028$$

- The central value is taken to be that of the current most precise measurement of the weak mixing angle.
- The systematic uncertainty is driven from lepton calibration (mainly forward calibration).
  - Significant contribution from experimental PDF uncertainties as well.
- Theory uncertainties arise from profiling different PDF sets and evaluating their impact.

Potential Weak Mixing Angle Sensitivity

Comparison to other Experiments

- The most precise measurements of the WMA are still from lepton colliders.
- CMS has published the most precise result from a hadron collider.
- This work is 20% more sensitive than the previous ATLAS 8 TeV measurement and 10% more precise than CMS!
- The estimated sensitivity is expected to reach lepton collider precision levels!

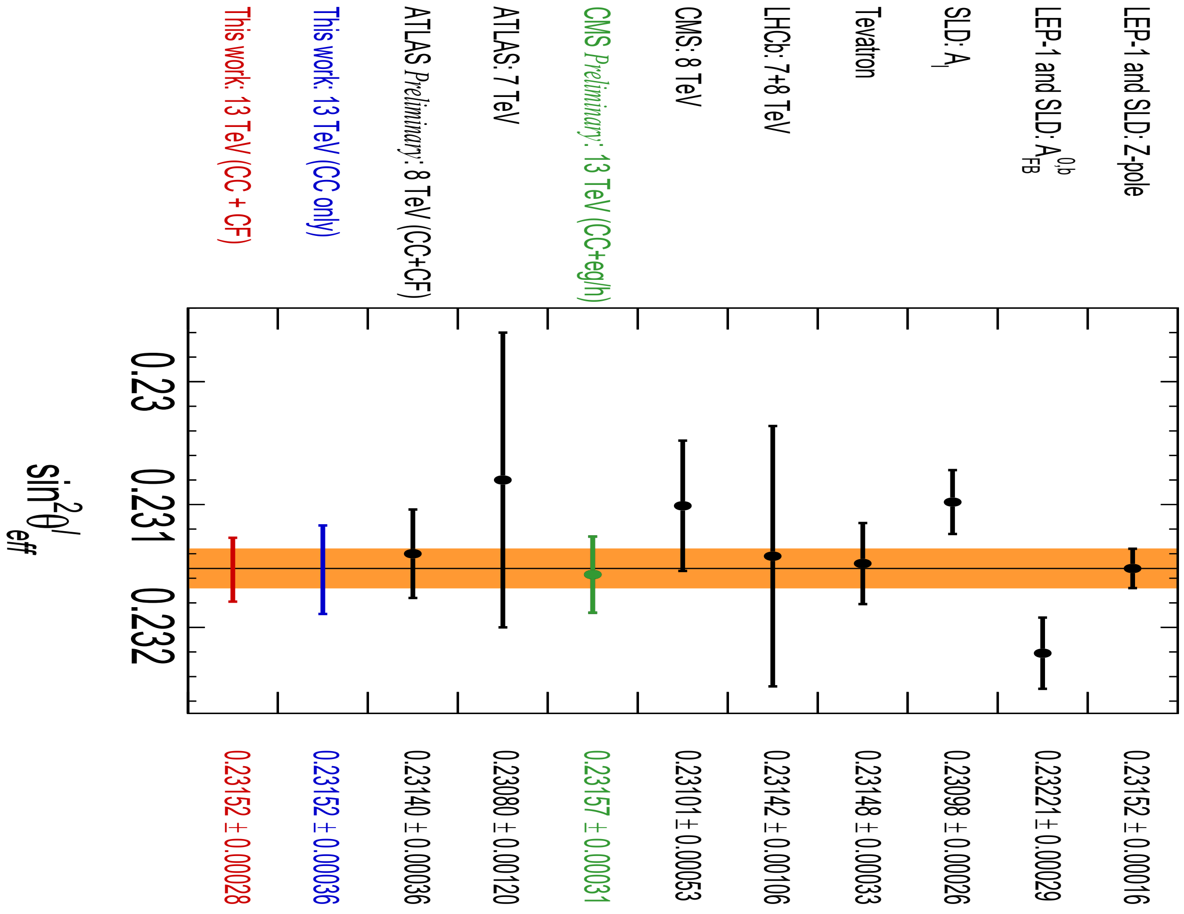

Summary

- Angular coefficients of the Z boson:
  - Measured at a much finer granularity and higher precision than ever before!
  - Behaviour compatible with the Standard Model is observed.
  - Potential non-compatibility with the Standard Model is observed in A_2 at low $p_{T,Z}$.

- New forward electron calibration chain:
  - MVA calibration to correct energy scale and improve resolution (20% in Monte Carlo, 10% in data).
  - Uniformity correction to correct for material effects and high voltage issues.
  - In situ correction that matches the data and Monte Carlo Z mass spectra.
  - Currently results in large systematic uncertainties but these can be improved!

- Asimov study on the sensitivity to the effective weak mixing angle:
  - Incorporate forward electrons into the analysis to maximise sensitivity.
  - By combining all three channels, the precision may reach 28×10^{-5}
  - 20% more sensitive than the previous ATLAS measurement and 10% more than the current best result from a hadron collider.

Backup

Collins-Soper Reference Frame

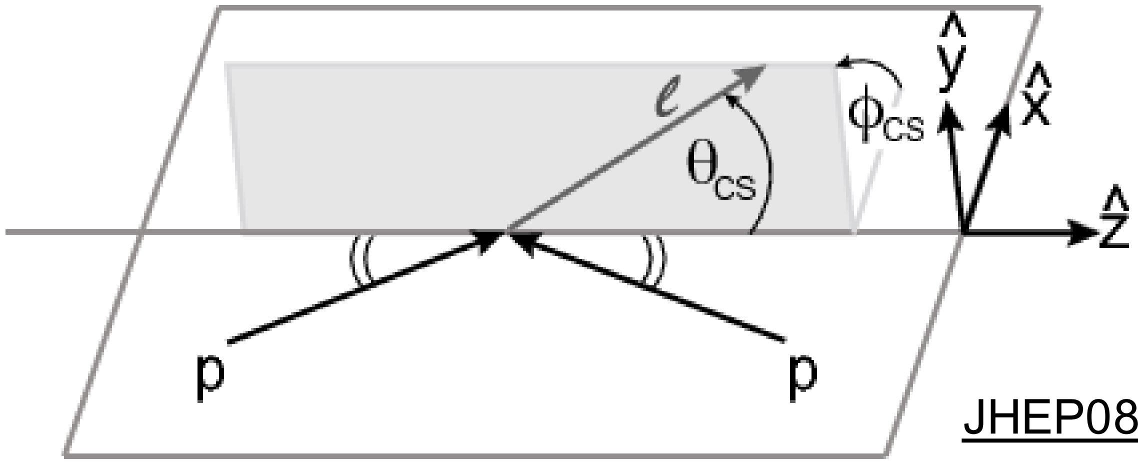

JHEP08(2016)159

- The CS frame is defined by two planes to form a right handed coordinate system:
  - The plane containing the colliding partons.
  - The perpendicular plane containing the decay lepton.
- The z-axis is taken to be in the direction of the quark.
- CS angles can be easily defined through lab frame quantities:

$$\cos\theta_{CS} = \frac{p_z^{ll}}{|p_z^{ll}|}\frac{(E_{l^-}+p_{z,l^-})(E_{l^+}-p_{z,l^+})-(E_{l^-}-p_{z,l^-})(E_{l^+}+p_{z,l^+})}{m_Z\sqrt{m_Z^2+p_{T,Z}^2}}$$

$$\sin\phi_{CS} = \frac{2}{\sin\theta_{CS}}\frac{p_{y,l^-}p_{x,l^+}-p_{y,l^+}p_{x,l^-}}{p_{T,Z}\,m_Z}$$

Interpretation of Angular Coeffcients

Coefficient	Meaning
A_0	Longitudinal polarisation fraction
A_1	Longitudinal-transverse polarisation interference
A_2	Transverse-transverse polarisation interference
A_3	Parity violation
A_4	Parity violation
A_5	Phase sensitive transverse-transverse interference
A_6	Phase sensitive longitudinal-transverse interference
A_7	Parity violation

Forward Electron Calibration

Uniformity Correction

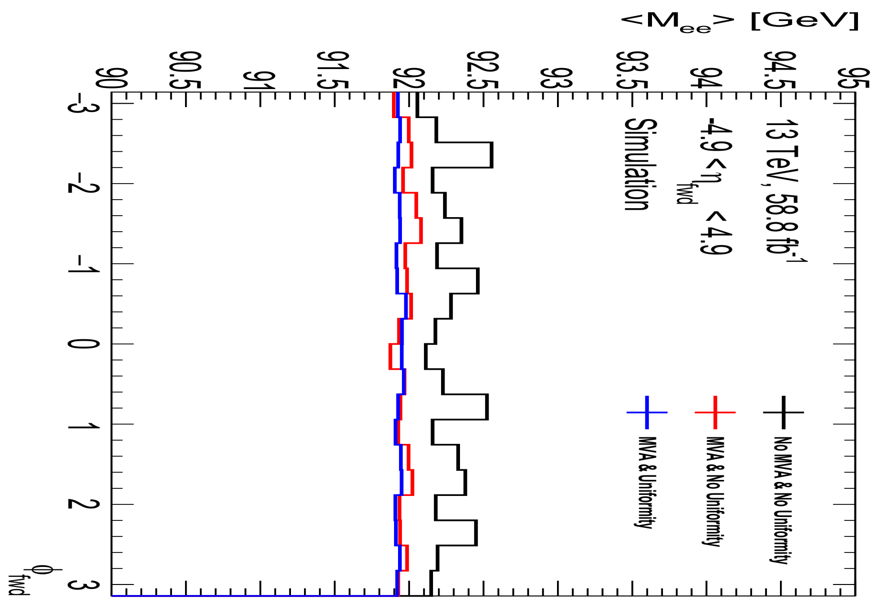

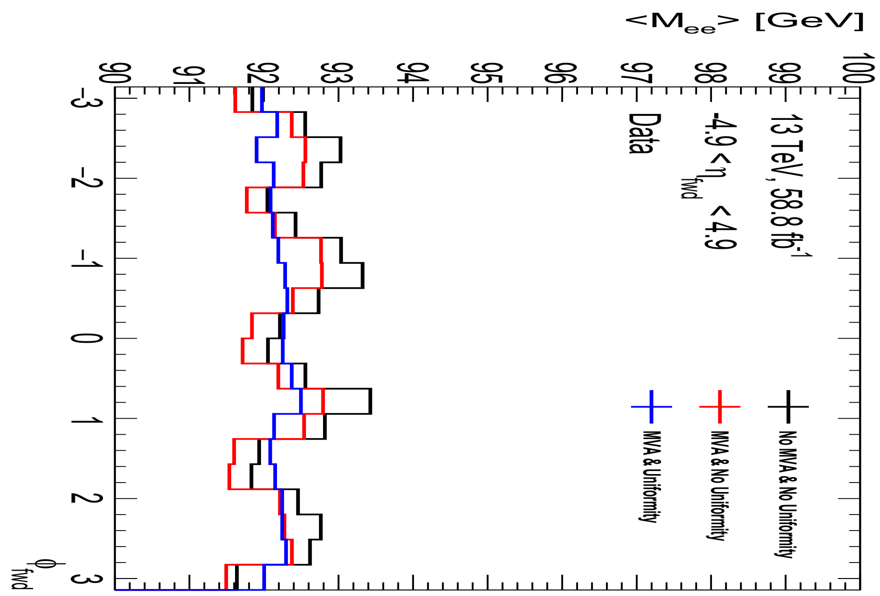

- The average mass of the reconstructed Z boson should not depend on the region of the detector being investigated!
- Passive material distributions and high voltage issues can affect electron energy reconstruction.
- The layout of passive material in the simulation does not match the real detector with 100% accuracy.
    - Post-MVA energy response is different between data and Monte Carlo!
    - Correct the uniformity separately for both cases.
- Correct electron energies in a single cell towards the median energy response of a given η slice.

Calculating Multijet Background

Fake Factor Method

Angular Coefficients

A_0 - Uncertainties

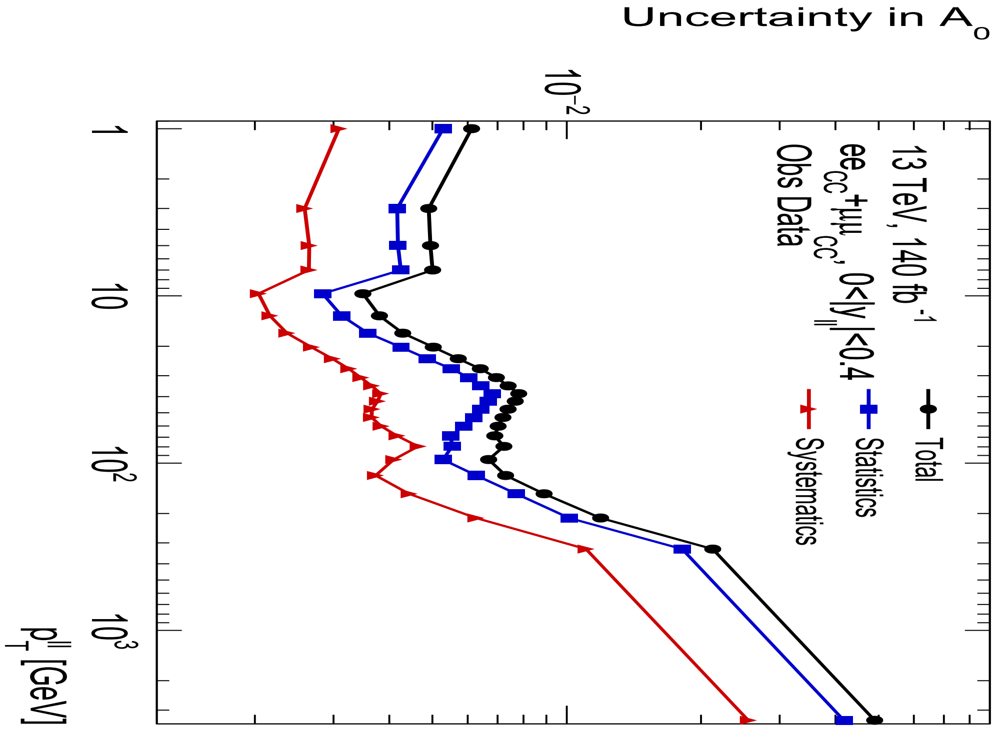

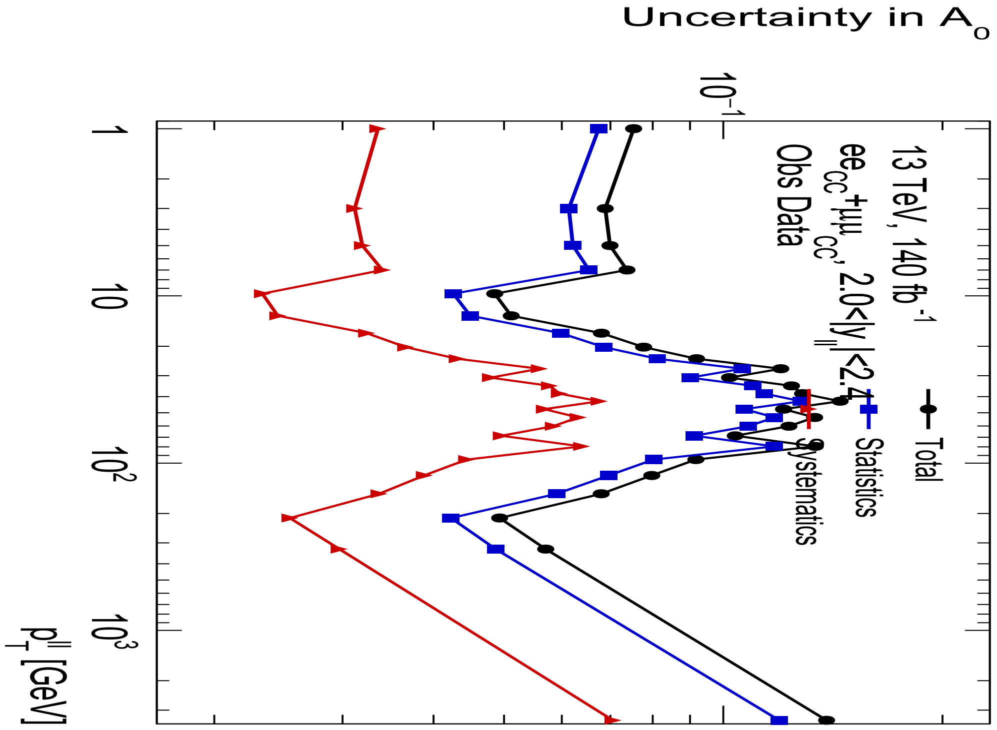

Angular Coefficients

A_2 - Uncertainties

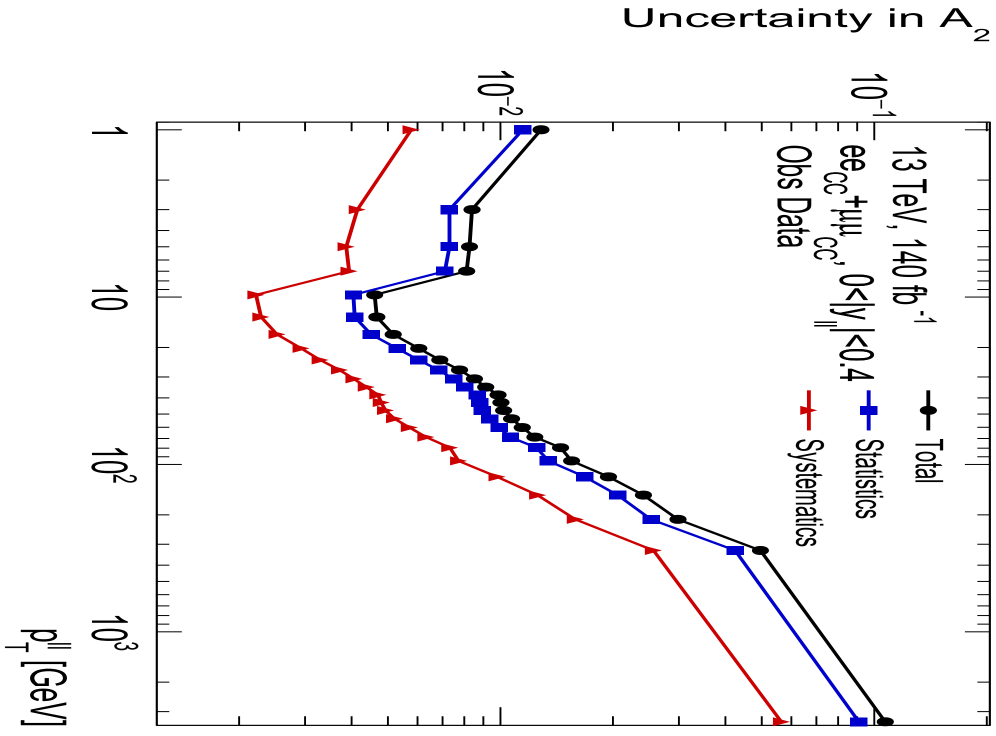

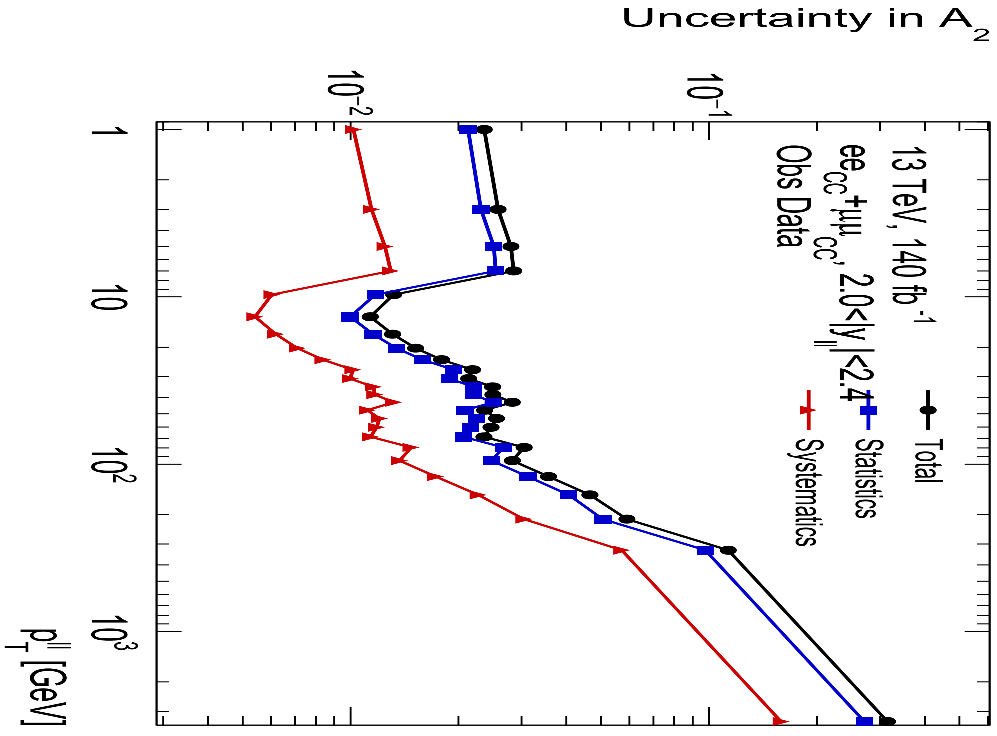

Angular Coefficients

A_3

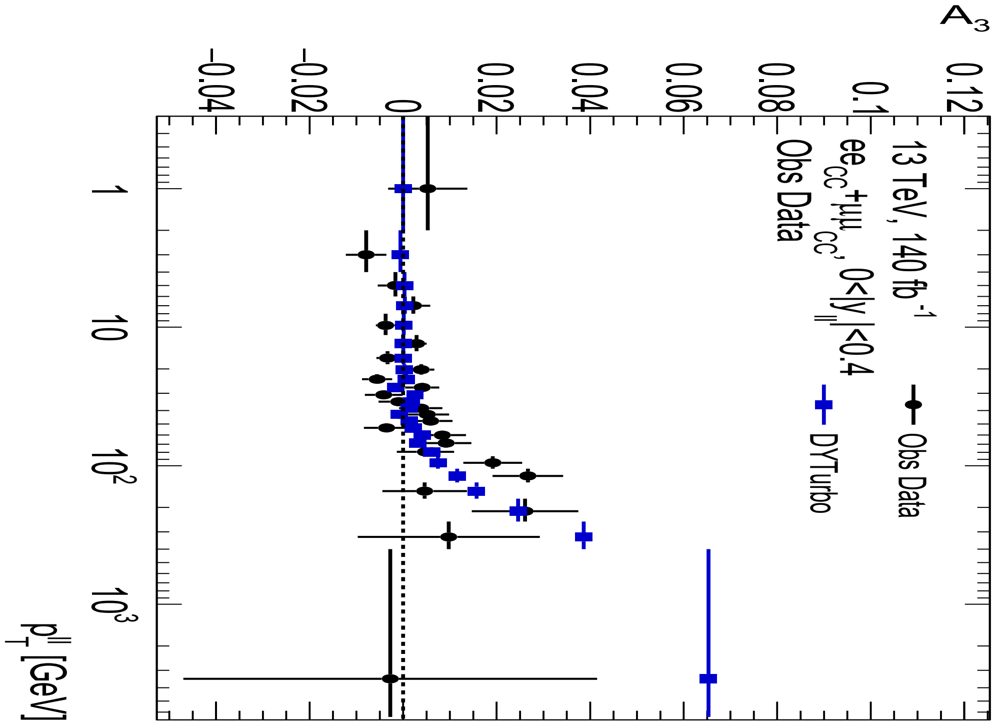

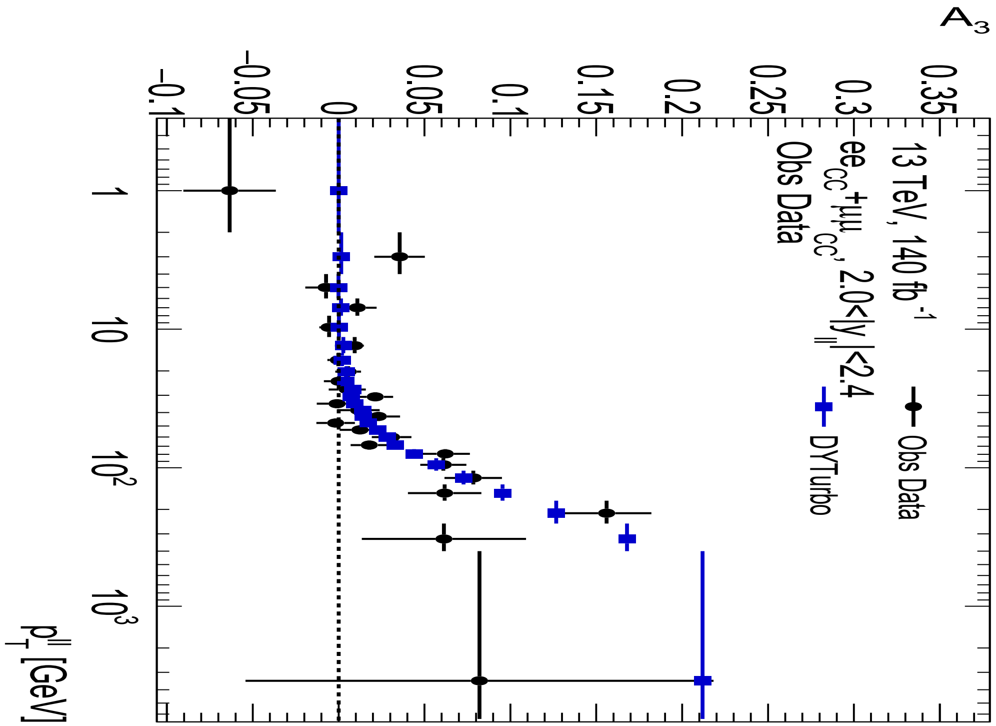

- First parity violating term in the decomposition.
- A_3 becomes non-zero only at high $p_{T,Z}$.
  - Overall contribution to A_{FB} is very small.
- Magnitude of A_3 increases with rapidity as is to be expected.

Angular Coefficients

A_3 - Uncertainties

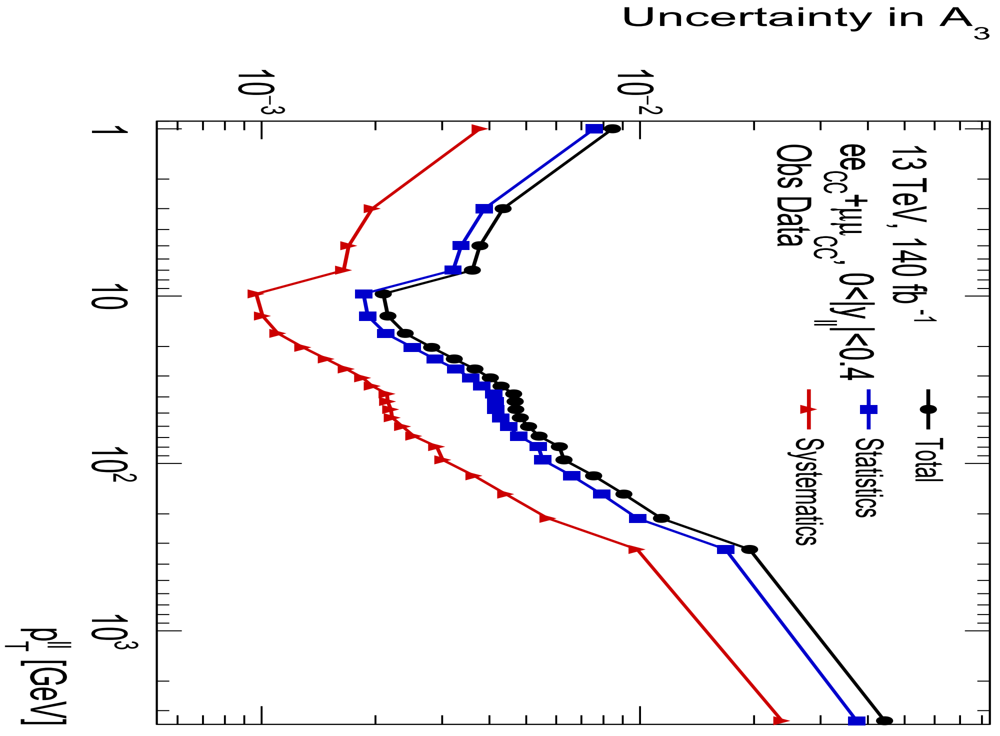

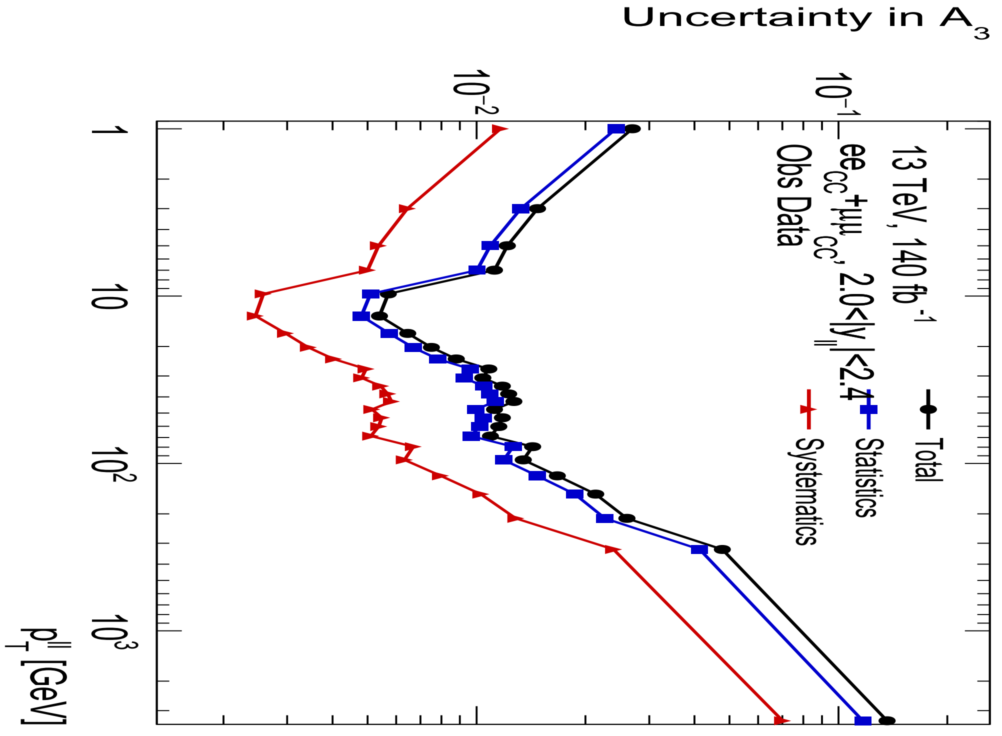

Angular Coefficients

A_4 - Uncertainties

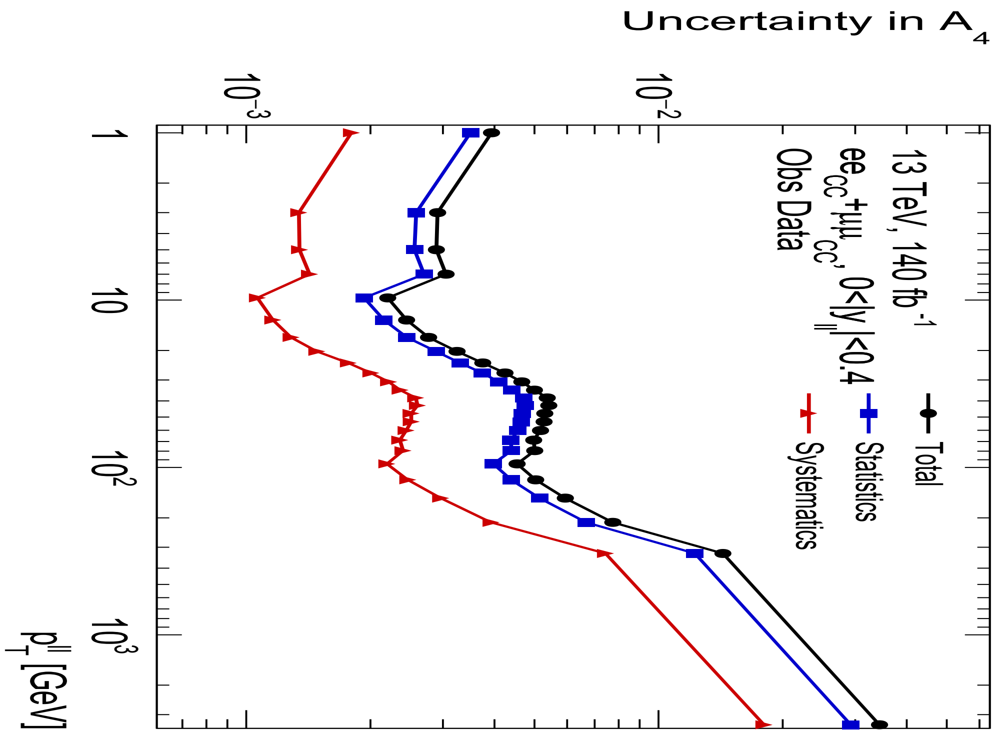

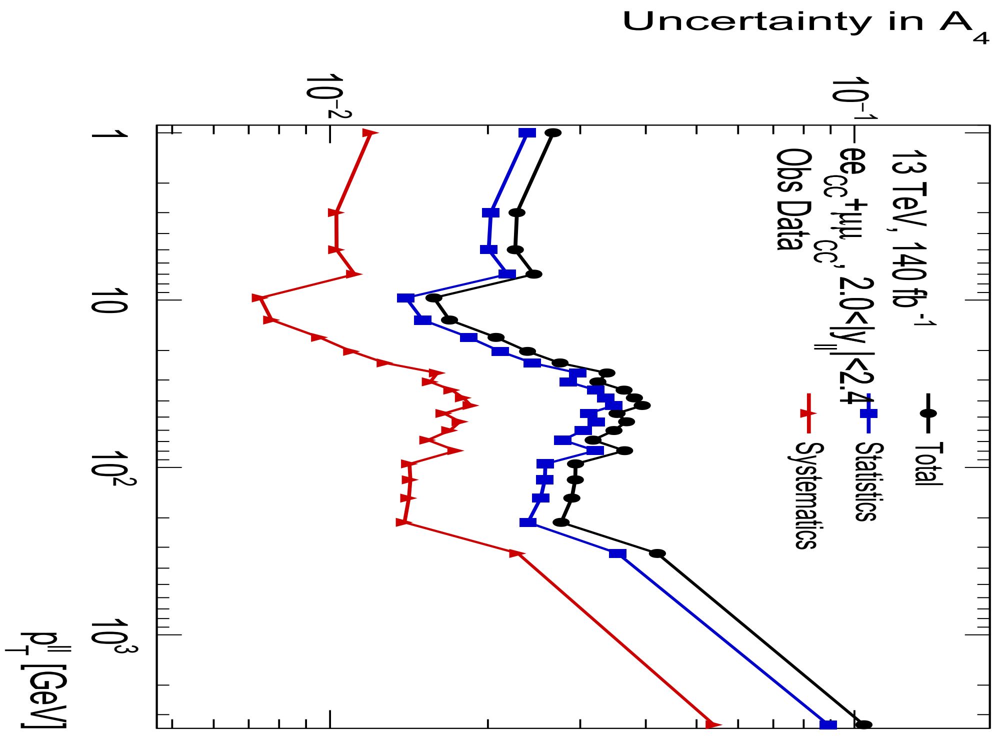

Angular Coefficients

Unpolarised Cross Section - Precision

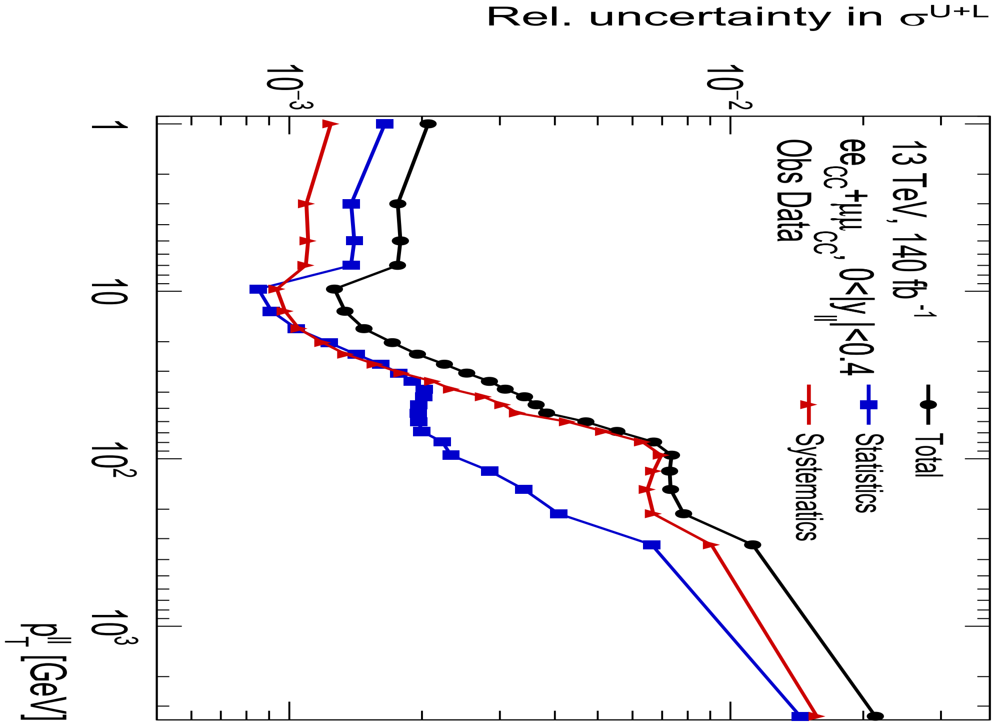

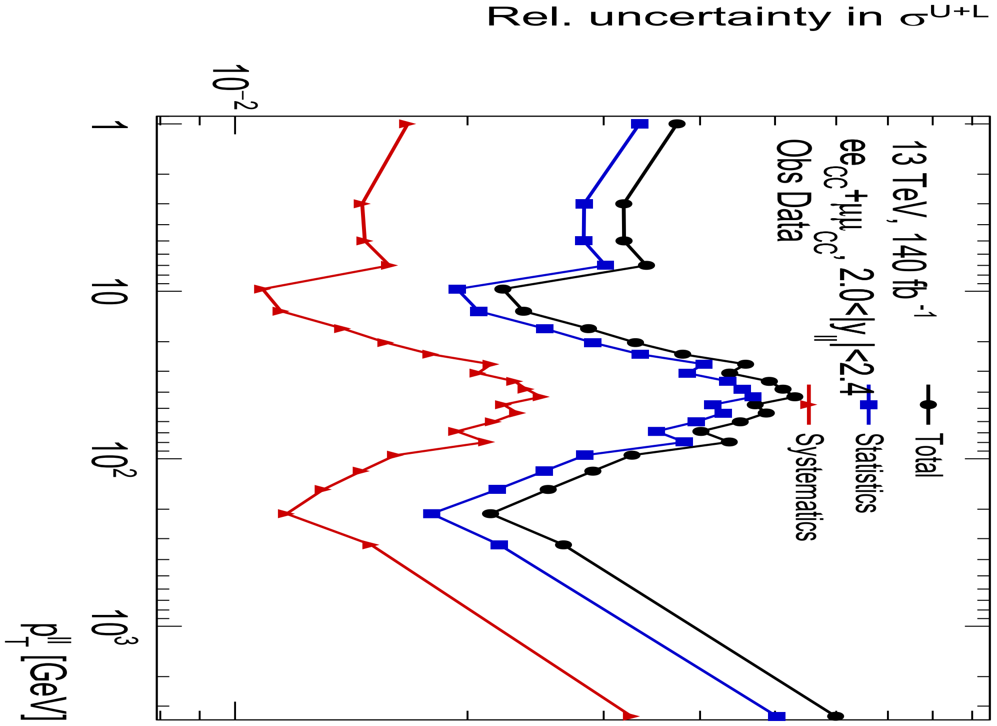

A_2 at Low Rapidity

Previous Measurements

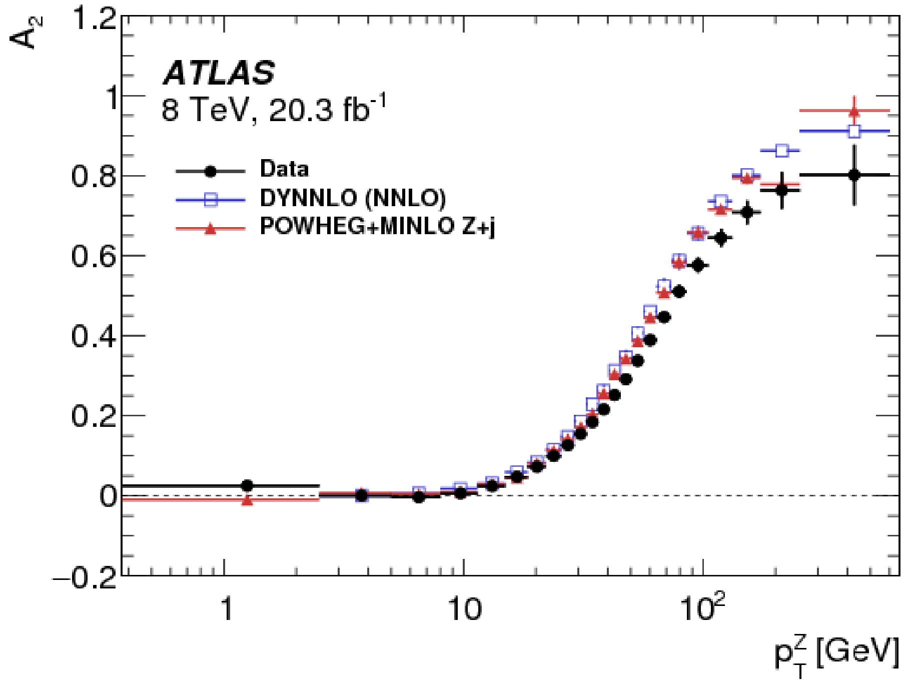

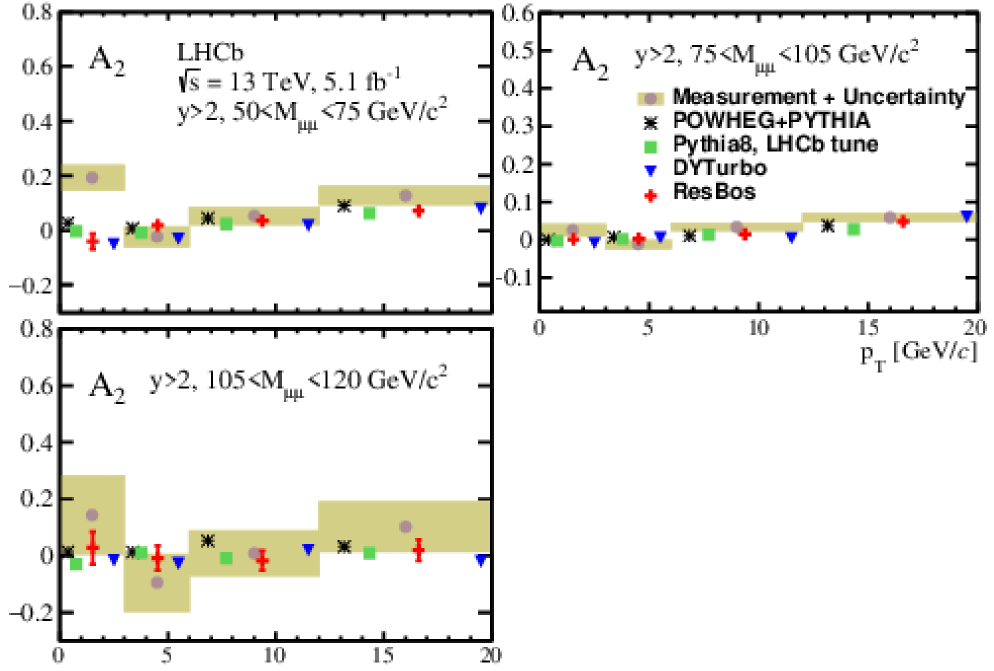

Forward Electron Calibration

MVA Input Variables

EMEC	FCal	Transition Region
E_{raw}	E_{raw}	E_{raw}
η_{cl}	Centre X/Y/Z	Centre X/Y/Z
ϕ_{cl}		
η mod $\Delta\eta$	η mod $\Delta\eta$	η mod $\Delta\eta$
Floor($\eta/\Delta\eta$)	Floor($\eta/\Delta\eta$)	Floor($\eta/\Delta\eta$)
μ	μ	μ
npv	npv	npv
$\langle r^2 \rangle$	$\langle r^2 \rangle$	-
$E_{S1,max}$ / $E_{S2,max}$	$\langle \rho^2 \rangle$	-
ϕ mod $2\pi/16$	λ_{centre}	-

Forward Electron Calibration

Shower Shape Corrections

Eur. Phys. J. C 77 (2017) 490

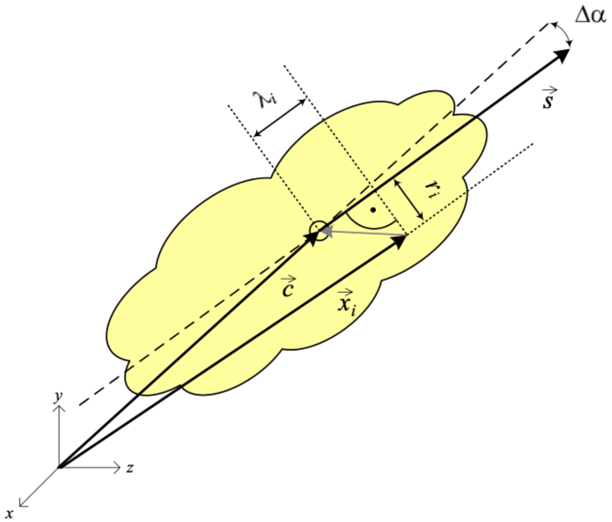

$\vec{c}$ *centre of gravity of cluster, measured from the nominal vertex* $(x = 0, y = 0, z = 0)$ *in ATLAS*

$\vec{x}_i$ *geometrical centre of a calorimeter cell in the cluster, measured from the nominal detector centre of ATLAS*

$\vec{s}$ *particle direction of flight (shower axis)*

$\Delta\alpha$ *angular distance* $\Delta\alpha = \angle(\vec{c}, \vec{s})$ *between cluster centre of gravity and shower axis* $\vec{s}$

λ_i *distance of cell at* $\vec{x}_i$ *from the cluster centre of gravity measured along shower axis* $\vec{s}$ $(\lambda_i < 0$ *is possible)*

r_i *radial (shortest) distance of cell at* $\vec{x}_i$ *from shower axis* $\vec{s}$ $(r_i \geq 0)$

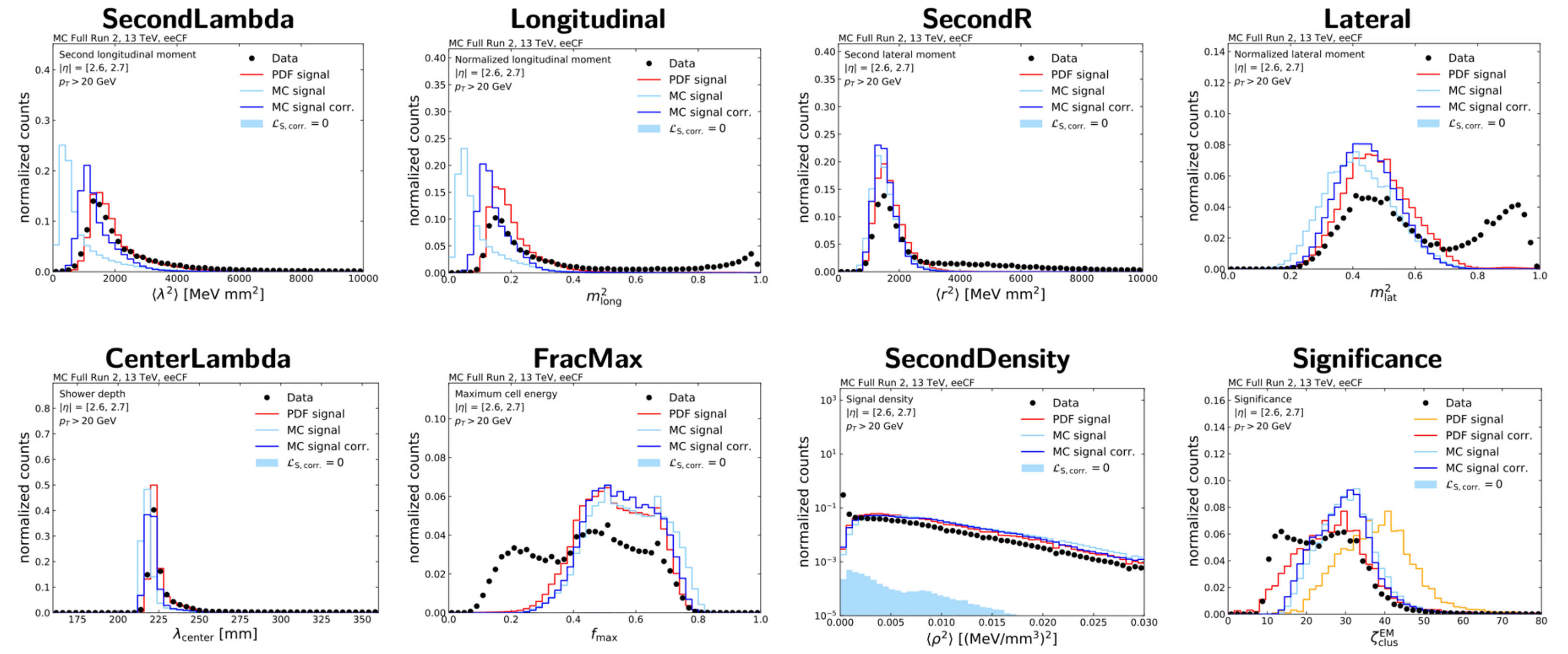

Shift and smear parameters are derived for each EMEC shower shape to move the signal distribution closer to the data.

M. Hohmann

Forward Electron Calibration

Double Sided Crystal Ball Definition

$$f(m;\mu,\sigma,\alpha_L,\alpha_U,n_L,n_U) = \begin{cases} A_L \times (B_L - \frac{m-\mu}{\sigma})^{-n_L} & \frac{m-\mu}{\sigma} < -\alpha_L \\ \exp\left(-\frac{(m-\mu)^2}{\sigma^2}\right) & -\alpha_L < \frac{m-\mu}{\sigma} < \alpha_U \\ A_U \times (B_U - \frac{m-\mu}{\sigma})^{-n_U} & \frac{m-\mu}{\sigma} > \alpha_U \end{cases}$$

$$A = \left(\frac{n}{|\alpha|}\right)^n \exp\left(\frac{-\alpha^2}{2}\right)$$

$$B = \frac{n}{|\alpha|} - |\alpha|$$

A_4 Results

Three Channel Combination

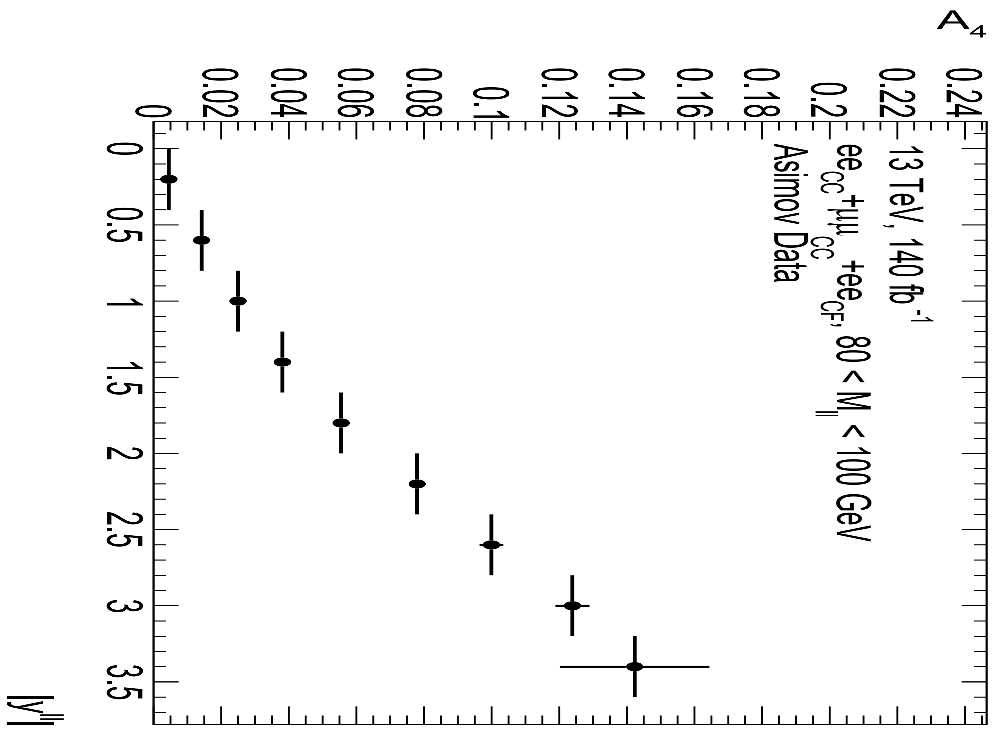

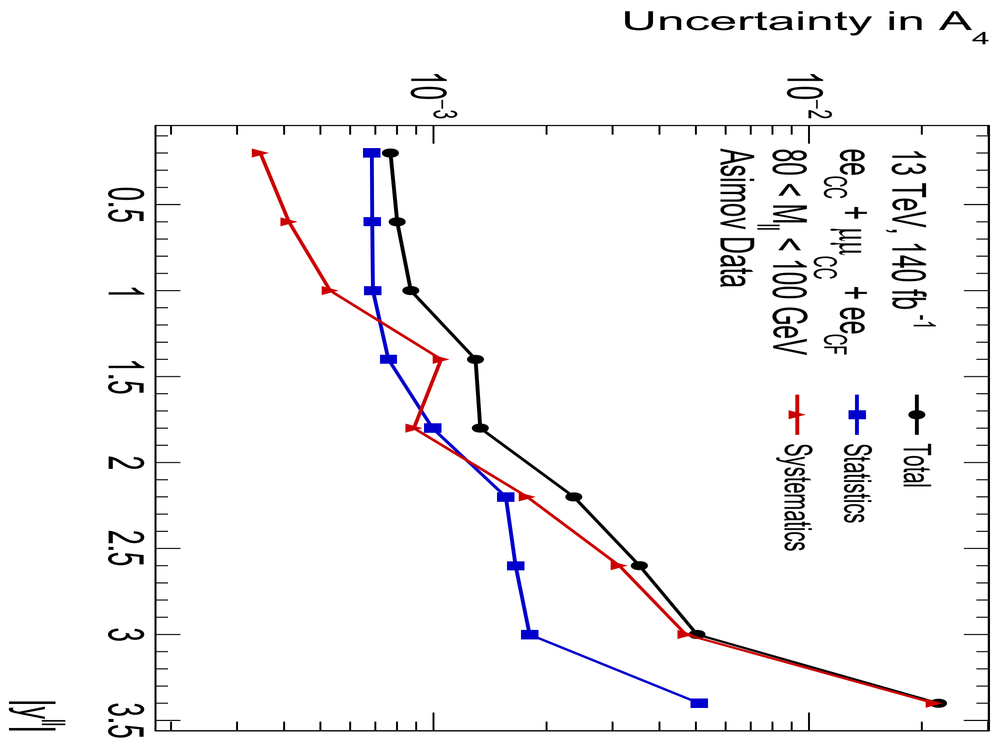

- Statistically limited at lower rapidities as systematics arise purely from the central channels.
- Systematically limited at higher rapidities due to the large uncertainties on the forward electron calibration.

Weak Mixing Angle Uncertainty Breakdown

Individual Channels

Uncertainty	Δee_{CC} (10^{-5})	ΔMM (10^{-5})	Δee_{CF} (10^{-5})
Statistical	44	34	36
MC Background	4	4	1
Central Electron Calibration	21	-	-
Muon Calibration	-	13	-
Forward Calibration	-	-	18
Central Lepton Efficiency	5	2	-
Forward ID Efficiency	-	-	5
Multijet Background	2	-	2
PDF (exp)	7	8	2
PDF (theory)	26	23	22
MC Stat	-	-	-
Total	56	44	46

Weak Mixing Angle Uncertainty Breakdown

Three Channel Combination

Uncertainty Source	Uncertainty (10^{-5})
MC Background	3
CC + MM Calibration	5
CF Calibration	6
Efficiency	2
Multijet	1
PDF (Experimental)	5
PDF (Theory)	14
Total Systematic	18
Statistical	22
Total	28

A_4 Dilution Between 8 and 13 TeV

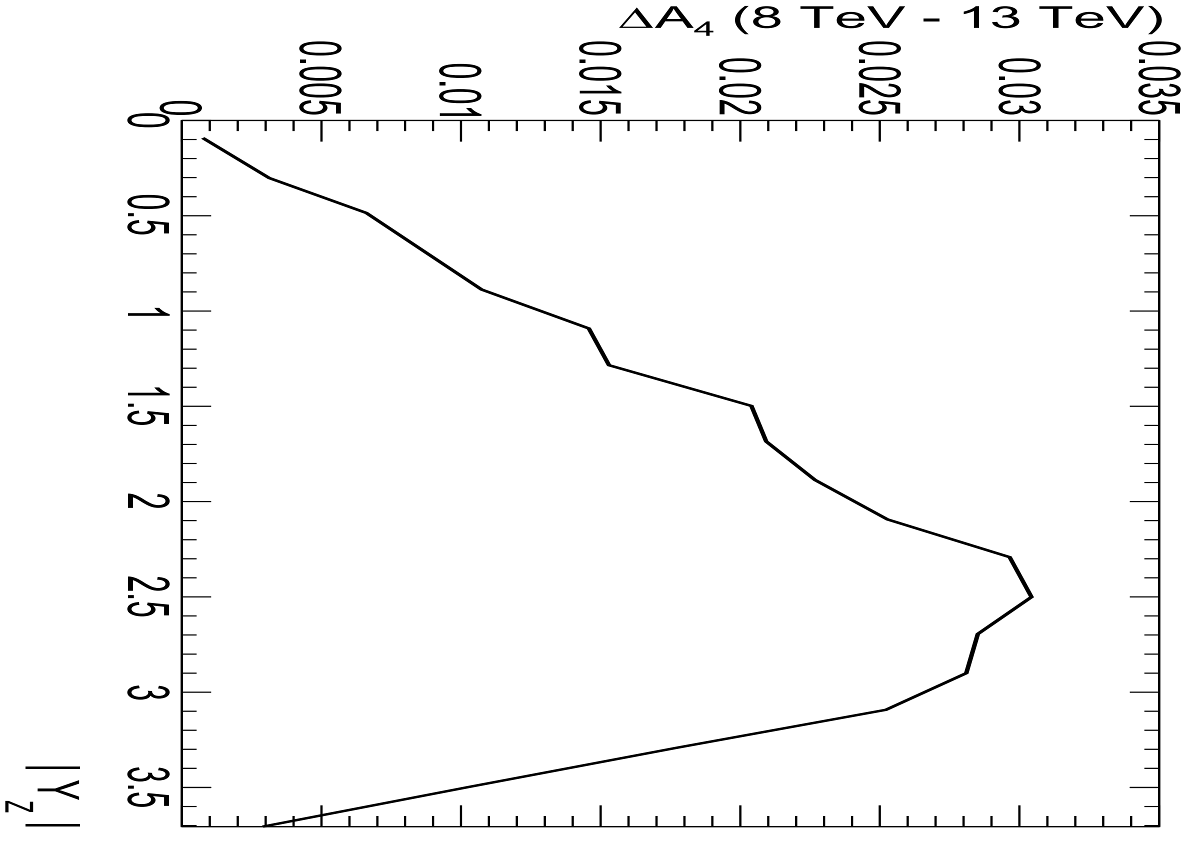

- Dilution affects A_4 the most in the CF region, meaning that a 13 TeV CF event loses more statistical power than a CC event.
- This has the effect of increasing the statistical uncertainty.